Spin liquid in an almost antiferromagnetic Kondo lattice

K. A. Kikoin, M. N. Kiselev, and A. S. Mishchenko

Kurchatov Institute, 123182 Moscow, Russia
(Submitted 2 January 1997)
Zh. Éksp. Teor. Fiz. **112**, 729–759 (August 1997)

A theory of stabilization of a spin liquid in a Kondo lattice at temperatures close to the temperature of antiferromagnetic instability has been developed. Kondo exchange scattering of conduction electrons leads to emergence of a state of the spin liquid of the resonating valence bonds (RVB) type at $T > T_K$. Owing to this stabilization, low-energy processes of Kondo scattering with energies below T_K are frozen so that the ''singlet'' state of the Kondo lattice is not realized; instead a strongly correlated spin liquid with developed antiferromagnetic fluctuations occurs. A new version of the Feynman diagram technique has been developed to describe interaction between spin fluctuations and resonant valence bonds in a self-consistent manner. Emergence of a strongly anisotropic RVB spin liquid is discussed. © *1997 American Institute of Physics.* [S1063-7761(97)02508-0]

1. INTRODUCTION

One of the most extraordinary properties of heavy-fermion compounds is the transition of a system of weakly interacting spins, which manifests paramagnetic properties at high temperatures, to a strongly correlated quantum liquid with thermodynamic and magnetic properties typical of Fermi systems at $T < T_{\rm coh} \ll T^*$. This ''dissolution'' of localized spins is usually interpreted in terms of the Kondo lattice model, and the basic mechanism which determines thermal transformation of the spin subsystem is assumed to be Kondo screening of spins by conduction electrons. This screening can be modeled in essentially the same way as a one-impurity lattice, so that the Kondo lattice can be treated as a periodic structure of Kondo impurities coherently scattering conduction electrons.[1,2] The characteristic temperature T^* at which the system switches to another regime is the Kondo temperature T_K, and the ground state in the mean-field approximation is the so-called Kondo singlet.

This simple model, however, ignores spin correlations, whose close relation to heavy fermions is beyond doubt. It is well known that formation of a heavy fermion is in all cases without exception due either to long-range antiferromagnetic order or short-range magnetic correlations. In its interpretation of this relation, the Kondo lattice theory invokes indirect exchange between localized spins via conduction electrons (RKKY exchange), which occurs in the Kondo lattice model in the second order of perturbation theory. Thus, nonlocal spin correlations compete with local effects of spin screening.[3] This naive dichotomy of Doniach's, which takes place in the mean-field approximation, predicts a tendency to antiferromagnetic ordering at small values of the effective coupling constant

$$\alpha = J_{sf}\mathcal{N}(\varepsilon_F)\Omega_0,$$

where J_{sf} is the sf-exchange integral, $\mathcal{N}(\varepsilon_F)$ is the electron density of states at the Fermi surface, Ω_0 is the elementary cell volume. At large α, Kondo screening suppresses the magnetic moment, and the ground state is the Kondo singlet. Then, for α slightly higher than α_c determined by the equation $\alpha_c^2 \exp(1/2\alpha_c) \approx 1$, the RKKY interaction can be calculated by perturbation theory, and magnetic correlations modify properties of the singlet phase.[4,5]

An alternative approach to the problem of competition between the one-site screening and magnetic intersite correlations was suggested by Coleman and Andrei.[6] The two options described by Doniach's simple model were supplemented with a third one, namely, formation of a nonmagnetic spin liquid of the resonant valence bonds (RVB) type with the Fermi statistics of elementary excitation in the spin system (spinons). They demonstrated that the spin liquid state is stabilized by Kondo scattering, but calculated both spin intersite correlations and the single-site sf-exchange between spinons and electrons in the mean-field approximation. Introduction of anomalous one-site averages of the Kondo type is, in reality, equivalent to the assumption that full dynamic spin screening takes place, and the assumption that Kondo singlets are formed at each site owing to multiple ''switching'' of RVB bonds between localized spins and conduction electron spins is equivalent to a translation of electron charge to spin degrees of freedom. Thus, in this scenario, as well as in the mean-field theory of the Kondo lattice,[7] spin degrees of freedom, which manifest themselves at high temperatures as weak paramagnetic, noncharged correlations, have a charge at $T < T_K$ and transform to charged heavy fermions (a critical discussion of this scenario was given in Ref. 8). Naturally, interpretation of the existence of magnetic correlations in the Kondo lattice requires more theoretical effort.[9]

This paper suggests an alternative scenario of formation of a spin liquid in the Kondo lattice described by the Hamiltonian

$$H_{\rm eff} = \sum_{\mathbf{k}\sigma} \varepsilon_k c^+_{\mathbf{k}\sigma} c_{\mathbf{k}\sigma} + J_{sf} \sum_{\mathbf{i}} \left(\mathbf{s_i}\cdot\mathbf{S_i} + \frac{1}{4} \right). \tag{1}$$

Here ε_k is the dispersion relation for conduction electrons, $\mathbf{S_i}$ and $\mathbf{s_i} = (1/2) c^+_{\mathbf{i}\sigma} \hat{\sigma} c_{\mathbf{i}\sigma}$, are operators of a spin localized in the f-shell and of a delocalized conduction electron spin, respectively, and $\hat{\sigma}$ are Pauli matrices. Our approach is based on an understanding that in the critical region, where all

three characteristic temperatures (the Kondo temperature $T_K \sim \varepsilon_F \exp(-1/2\alpha)$, Néel temperature $T_N \sim \varepsilon_F \alpha^2$, and the temperature T^* of the transition to the spin-liquid state) are of the same order, and the Kondo scattering is favorable to the transition to the spin-liquid state so that $T^* > T_N > T_K$, the very existence of spin-liquid correlations impedes the formation of a singlet ground state, since screening of localized spins by the Kondo scattering is, in fact, frozen at temperatures $T \sim T^* > T_K$, and at lower temperatures the system properties are controlled by nonlocal spin-liquid correlations, rather than one-site Kondo scattering. In other words, spin correlations suppress the Kondo effect in both the ordered (magnetic) and disordered (spin-liquid) phases, so Doniach's simple phase diagram should be revised.

Since the spin-liquid state emerges in the critical region $\alpha \sim \alpha_c$ at temperatures close to T_N, the coexistence of heavy fermions and magnetic correlations has a natural interpretation in the proposed model. Moreover, it is obvious that critical spin fluctuations should play an important role in the mechanism of spin-liquid formation. In this study, we have limited our calculations to the range of high temperatures $T > T_K$, where the perturbation theory in the parameter $\alpha \ln(\varepsilon_F/T_K)$ applies. We use the diagram technique for spin operators in the pseudofermion representation[10] in the approximation of noncrossing graphs (or noncrossing approximation, NCA) for the description of the Kondo scattering. The results of high-temperature expansions, which take one-site and intersite correlations into account concurrently, will be extrapolated to the range of temperatures where paramagnetic fluctuations are important. However, when the pseudofermion technique is applied to nonlocal spin-liquid correlations, the problem of nonphysical states arises, and hence the breaking of local spin symmetry.[11–15] With this circumstance in view, we have constructed a Feynman diagram technique for spin Hamiltonians, which allows us, in principle, not only to get rid of nonphysical states, but also to take into account fluctuations of calibration fields.

In Sec. 2 this technique is applied to a spin liquid of the homogeneous RVB phase type[16,17] described in terms of the Heisenberg model; in Sec. 3 the technique is applied to the Kondo lattice, and the mechanism of RVB phase stabilization by Kondo scattering in the mean-field approximation is described.[1)] The mean-field theory for the RVB phase, taking into account critical fluctuations, is generalized in Sec. 4, and Sec. 5 shows how this diagram technique can be used in describing local critical and hydrodynamic fluctuations around the antiferromagnetic instability point.

2. PROJECTION DIAGRAM TECHNIQUE FOR THE HEISENBERG LATTICE

Along with standard perturbation theory techniques developed for Fermi and Bose operators, one can find in the literature a number of diagram techniques for noncommuting operators in terms of which one can write the Hamiltonians of the spin or strongly correlated electrons systems (see, for example, Refs. 19–21 and references therein). Most of these techniques are based on Hubbard's projection operators $X_{\mathbf{j}}^{\lambda\mu} = |\mathbf{j}\lambda\rangle\langle\mathbf{j}\mu|$, where $|\mathbf{j}\lambda\rangle$ is a ket vector corresponding to state λ at site j, and the Hamiltonian in the zeroth order of perturbation theory is diagonalized in this approximation.

Diagram techniques for noncommuting operators are harder to handle than the standard Feynman technique. Only in some cases do they allow a self-consistent form of closed equation systems for skeleton diagrams. Goden's procedure factorizing the average of n operators, unlike Wick's procedure, which plays a similar role in the usual diagram technique, is ambiguous, and a successful choice of the hierarchy of couplings largely depends on the theorist's intuition (see, for example, Ref. 22).

For this reason, it is natural to attempt to express Hubbard's operators (and spin operators, which are a special case of these operators) as products of Fermi and Bose operators, and thus restore conditions for using the machinery of the Feynman and Matsubara techniques. Such attempts have been undertaken many times since the 1960s,[10,23–25] up through recent times.[22,26–28] It is clear, however, that these procedures are by no means universal or unambiguous. Moreover, each factorization leads to multiplication and complication of vertices and emergence of local constraints, whose introduction is necessary for the preservation of local gauge invariance, which is a trait of the Hamiltonian in question.

Additional problems arise due to attempts to describe nonlocal spin-liquid RVB excitation. In this case, problems arise on the level of the mean-field approximation for the self-energy part of the one-particle propagator. The usual techniques of self-consistent perturbation theory break the local gauge invariance,[11] and its restoration is quite a difficult physical and mathematical problem.[13,14]

In this section we formulate a version of the diagram technique integrating the two approaches mentioned above, and apply it to Hamiltonians with local SU(2) symmetry. With a view toward using this technique in the description of spin liquid in terms of Hamiltonian (1), we start with the simpler case of the Heisenberg Hamiltonian for spin 1/2 with antiferromagnetic interaction:

$$H = h\sum_{\mathbf{i}} S_{\mathbf{i}}^z + J\sum_{\mathbf{i}} \sum_{\mathbf{j}}^{\langle nn\rangle} \left(\mathbf{S_i}\cdot\mathbf{S_j} - \frac{1}{4} \right); \tag{2}$$

we then pass to a description of the Kondo lattice at high temperatures $T > T_K$, for which the noncrossing approximation (NCA) applies, and the system can be treated as a periodic lattice of independent Kondo scatterers interacting via the RKKY mechanism.[3]

Let us introduce a pseudofermion representation[10] for spin operators:

$$S^+ = f_\uparrow^+ f_\downarrow, \quad S^- = f_\downarrow^+ f_\uparrow, \quad S^z = \frac{1}{2}(f_\uparrow^+ f_\uparrow - f_\downarrow^+ f_\downarrow). \tag{3}$$

These operators satisfy the local constraint condition

$$n = f_\uparrow^+ f_\uparrow + f_\downarrow^+ f_\downarrow = 1 \tag{4}$$

at each site. The first term in Eq. (2) describes Zeeman splitting in an infinitesimal magnetic field $h = g\mu_B H$, and the antiferromagnetic sign of the exchange constant J is taken into account explicitly.

The SU(2) invariance means that the spin operators $\{S^+,S^-,S^z\}$ can be expressed as arbitrary linear combinations of spin-fermions $\{f_\uparrow,f_\downarrow,f_\uparrow^+,f_\downarrow^+\}$:

$$S_{\mathbf{i}}^+=(\cos\,\theta f_{\mathbf{i}\uparrow}^+ +\sin\,\theta f_{\mathbf{i}\downarrow}\,)(\cos\,\theta f_{\mathbf{i}\downarrow}-\sin\,\theta f_{\mathbf{i}\uparrow}^+\,),$$

$$S_{\mathbf{i}}^-=(\cos\,\theta f_{\mathbf{i}\downarrow}^+ -\sin\,\theta f_{\mathbf{i}\uparrow})(\cos\,\theta f_{\mathbf{i}\uparrow}+\sin\,\theta f_{\mathbf{i}\downarrow}^+), \tag{5}$$

$$S^z=\frac{1}{2}(f_{\mathbf{i}\uparrow}^+ f_{\mathbf{i}\uparrow}-f_{\mathbf{i}\downarrow}^+ f_{\mathbf{i}\downarrow}).$$

In particular, for pseudofermion filling factors, we have complete particle–hole symmetry,

$$f_{\mathbf{i}\sigma}^+ f_{\mathbf{i}\sigma}=f_{\mathbf{i}-\sigma}f_{\mathbf{i}-\sigma}^+, \tag{6}$$

which directly follows from condition (4) or from Eqs. (5) for $\theta = 0,\pi/2$. Thus, Hamiltonian (2) can be expressed in the pseudofermion representation as

$$H=H_0+H_{\rm int}=-\frac{h}{2}\sum_{\mathbf{i}\sigma}\,\sigma f_{\mathbf{i}\sigma}^+ f_{\mathbf{i}\sigma}+\frac{J}{2}\sum_{\mathbf{ij}\sigma}\,f_{\mathbf{i}\sigma_1}^+ f_{\mathbf{j}\sigma_1}f_{\mathbf{j}\sigma_2}^+ f_{\mathbf{i}\sigma_2}. \tag{7}$$

The local constraint places significant limits on the feasibility of using standard diagrammatic techniques, or in any case, makes more difficult practical description of the spin dynamics in the fermion representation, since the functional space in which the spin and fermion operators act has finite dimensionality. One of the most convenient techniques for including the spin kinetamics in the fermion representation was suggested by Abrikosov.[10] $2S+1$ spins (projections) correspond to a localized spin $\mathbf{S_i}$, whereas in its description in terms of pseudofermion operators $2^{(2S+1)}$ orthogonal states emerge, in accordance with the filling numbers (0,1) for all $2S+1$ spin projections. In a specific case of spin $S = 1/2$, there are four fermion states:

$$|0\rangle=|0,0\rangle;\quad |+\rangle=|1,0\rangle;\quad |-\rangle=|0,1\rangle;\quad |2\rangle=|1,1\rangle \tag{8}$$

and only two of them, namely states $|\pm\rangle$, correspond to physical states of the spin operator. Abrikosov suggested ascribing energy $\lambda \gg T$ to each state occupied by a pseudofermion. Then the nonphysical state $|2\rangle$ from set (8) is frozen out after averaging owing to the additional factor $\exp(-\lambda/T)$ in the partition function $\mathcal{Z}(T)$. In order to get rid of the other nonphysical state $|0\rangle$, one must introduce an additional factor $(1/2)\exp(\lambda/T)$ to $\mathcal{Z}(T)$ and take the limit $\lambda/T\to\infty$ in averaging over spin states. As a result, physical states $|\pm\rangle$ become states with the lowest ''energy'', and the final result is independent of λ. Abrikosov's prescription applies to local spin states in the case of a one-impurity Hamiltonian of sf-exchange. In a Kondo lattice it can be used only in the limit of large spin with degeneracy $N\to\infty$, for which NCA becomes an asymptotically exact approximation,[29] but this technique cannot be used in describing spin-liquid correlations.

The starting point of the proposed method is the well known similarity between the Heisenberg and Hubbard Hamiltonians in the limit of strong interaction U in the case of half-filled states. Let us express pseudofermion operators in the form of sums,

$$f_{\mathbf{i}\sigma}^+=f_{\mathbf{i}\sigma}^+(1-n_{\mathbf{i}-\sigma})+f_{\mathbf{i}\sigma}^+ n_{\mathbf{i}-\sigma},$$

$$n_{\mathbf{i}\sigma}=n_{\mathbf{i}\sigma}(1-n_{\mathbf{i}-\sigma})+n_{\mathbf{i}\sigma}n_{\mathbf{i}-\sigma}, \tag{9}$$

and introduce Hubbard's projection operators for pseudofermions, as was done by Hubbard for the real electron operators[30]:

$$X_{\mathbf{i}}^{\sigma 0}=f_{\mathbf{i}\sigma}^+(1-n_{\mathbf{i}-\sigma}),\quad X_{\mathbf{i}}^{2\sigma}=-\sigma f_{\mathbf{i}-\sigma}^+ n_{\mathbf{i}\sigma},$$

$$X_{\mathbf{i}}^{\sigma\sigma}=n_{\mathbf{i}\sigma}(1-n_{\mathbf{i}-\sigma})=n_{\mathbf{i}\sigma}n_{\mathbf{i}-\sigma},\quad X_{\mathbf{i}}^{22}=n_{\mathbf{i}\uparrow}n_{\mathbf{i}\downarrow},$$

$$X_{\mathbf{i}}^{00}=(1-n_{\mathbf{i}\uparrow})(1-n_{\mathbf{i}\downarrow}), \tag{10}$$

$$X_{\mathbf{i}}^{\sigma-\sigma}=f_{\mathbf{i}\sigma}^+ f_{\mathbf{i}-\sigma}=X_{\mathbf{i}}^{\sigma 2}X_{\mathbf{i}}^{2-\sigma}=X_{\mathbf{i}}^{\sigma 0}X_{\mathbf{i}}^{0-\sigma}.$$

These operators form a normalized basis for the group SU(4) with the obvious completeness condition

$$\sum_\mu X_{\mathbf{i}}^{\mu\mu}=1. \tag{11}$$

The second line of Eq. (9) can be rewritten in the form

$$n_{\mathbf{i}\sigma}=X_{\mathbf{i}}^{\sigma 0}X_{\mathbf{i}}^{0\sigma}+X_{\mathbf{i}}^{\sigma 2}X_{\mathbf{i}}^{2\sigma}. \tag{12}$$

As a result, Hamiltonian (2), (7) takes the form

$$H=H_0+H_{\rm int},$$

$$H_0=-\frac{h}{2}\sum_{\mathbf{i}\sigma}\,\sigma X_{\mathbf{i}}^{\sigma\sigma}+\frac{U}{2}\sum_{\mathbf{i}}\,(X_{\mathbf{i}}^{00}+X_{\mathbf{i}}^{22}), \tag{13}$$

$$H_{\rm int}=\frac{J}{2}\sum_{\mathbf{ij}\sigma}\,(X_{\mathbf{i}}^{\sigma-\sigma}X_{\mathbf{j}}^{-\sigma\sigma}-X_{\mathbf{i}}^{\sigma\sigma}X_{\mathbf{j}}^{-\sigma-\sigma})$$

$$=\frac{J}{2}\sum_{\mathbf{ij}\sigma\sigma'}\,\phi_{\mathbf{ij}}^{\sigma}\phi_{\mathbf{ji}}^{\sigma'}.$$

Here

$$\phi_{\mathbf{ij}}^{\sigma}=(\sigma X_{\mathbf{i}}^{2-\sigma}+X_{\mathbf{i}}^{\sigma 0})(\sigma X_{\mathbf{j}}^{-\sigma 2}+X_{\mathbf{j}}^{0\sigma}), \tag{14}$$

and the fictitious Hubbard repulsion parameter U for pseudofermions is introduced so as to preserve the particle–hole symmetry of the Heisenberg Hamiltonian.

Instead of using diagram techniques for the X-operators (see, for example, Refs. 19, 22, 31, and 32), we try to remain within the standard Feynman approach, but use the properties of the projection operators $X_{\mathbf{i}}^{\lambda\mu}$ in explicit form. We take for a basis of the diagram expansion the eigenstates of the Hamiltonian H_0 under the condition $U/T \equiv \beta U\to\infty$. As a result, we have the reduced Hamiltonian

$$\widetilde{H}=\widetilde{H}_0+H_{\rm int},\quad \widetilde{H}_0=-\frac{h}{2}\sum_{\mathbf{i}\sigma}\,\sigma f_{\mathbf{i}\sigma}^+ f_{\mathbf{i}\sigma} \tag{15}$$

with the partition function $\hat{\mathcal{Z}} = \mathrm{Tr}[\exp(-\beta\widetilde{H})]$, which includes only physical states $|\sigma\rangle = |\pm\rangle$ from set (8). The Hamiltonian H_0 reduces to $\widetilde{H}_0$ since the operators $X_{\mathbf{i}}^{\sigma\sigma}$ and $f_{\mathbf{i}\sigma}^+ f_{\mathbf{i}\sigma}$ have identical matrix elements in the reduced (physical) space. Now we can use $\widetilde{H}$ in the form (15) as a zero-approximation Hamiltonian for the Matsubara diagram technique.[2)]

Selection of one of the two forms of Hamiltonian (13) depends on which of the spin system states we are going to describe. Whereas the most convenient representation for the high-temperature paramagnetic phase or a state with long-

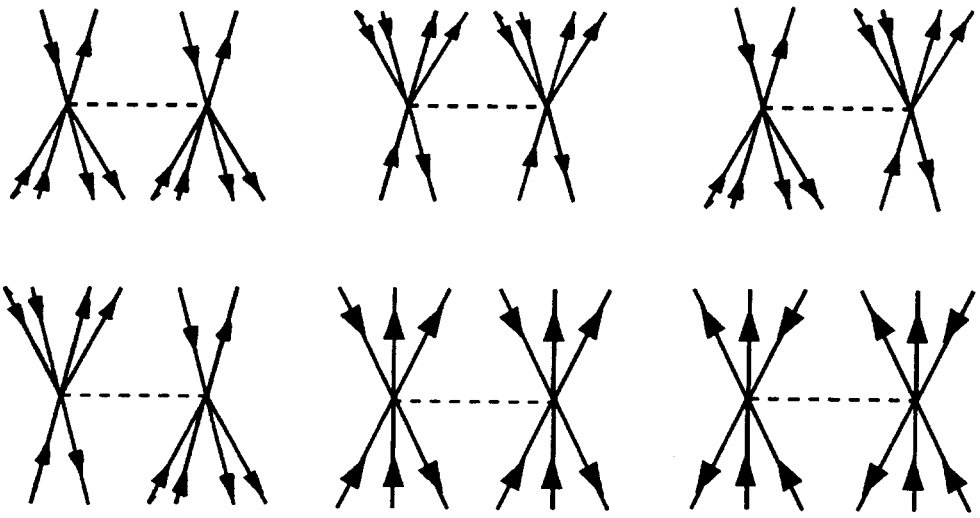

FIG. 1. Bare exchange vertices with due account of projection operators.

range magnetic order is $H_{\rm int}$ in terms of spin operators $X_{\mathbf{i}}^{\sigma\sigma'}$, it is natural to describe the RVB spin-liquid state in terms of operators $\phi_{\mathbf{ij}}^{\sigma}$.

Let us first consider the temperature Green's function

$$\mathscr{K}_{\mathbf{ij}}^{\perp}(\tau)=\langle T_{\tau}S_{\mathbf{i}}^{+}(\tau)S_{\mathbf{j}}^{-}(0)\rangle_{\tilde{H}}, \tag{16}$$

which describes elementary excitations in the standard theory of magnetism ($i\tau$ is the imaginary ''time''). To zeroth-order in the interaction, the function has the form

$$\mathscr{K}_{\mathbf{ij}}^{0}(\tau)=\frac{\delta_{\mathbf{ij}}}{4}\langle T_{\tau}f_{\mathbf{i}\uparrow}^{+}(\tau)f_{\mathbf{i}\downarrow}(\tau)f_{\mathbf{i}\downarrow}^{+}(0)f_{\mathbf{i}\uparrow}(0)\rangle_{\tilde{H}_0}. \tag{17}$$

Averaging is performed with the partition function $\mathscr{Z}=2\cosh(\beta h)$, $\beta=1/kT$. In accordance with Wick's theorem, this average can be presented in the form of a two-fermion loop and reduces to the simple expression

$$\mathscr{K}_{\mathbf{ij}}^{0}(\tau)=\frac{\delta_{\mathbf{ij}}}{4}e^{-h\tau}\begin{cases}\langle n_{\mathbf{i}\uparrow}(1-n_{\mathbf{i}\downarrow})\rangle_{\tilde{H}_0} & (\tau>0)\\ \langle n_{\mathbf{i}\downarrow}(1-n_{\mathbf{i}\uparrow})\rangle_{\tilde{H}_0} & (\tau<0)\end{cases}. \tag{18}$$

One can see that by virtue of Eq. (4), fermion states are generated in pairs, and the emergence of filling factors in the form of averages of projection operators $\langle X^{\sigma\sigma}\rangle_{\tilde{H}_0}$ [see Eq. (10)] shows that spin operators do not drive the system from the space of ''physical'' states $|\pm\rangle$.

Thus, the limit $U\to\infty$ for effective Hamiltonian (13) is equivalent to the limit $\lambda\to\infty$ in Abrikosov's procedure described above, which ''freezes out'' nonphysical pseudofermion states $|0\rangle$ and $|2\rangle$ without breaking the particle–hole symmetry.

The perturbation theory series for the function $\mathscr{K}^{\perp}$ can be constructed in accordance with the usual rules for calculating two-time Green's functions. This procedure leads to Larkin's equation[34]

$$\mathscr{K}=\Sigma+J\Sigma.\mathscr{K}. \tag{19}$$

Here Σ is the irreducible polarization operator, which is not separable with respect to the interaction. In Sec. 5 we will use this version of the diagram technique to calculate the spin diffusion coefficient near the Néel point.

Let us proceed to nonlocal spin-liquid correlations. We consider as an example an RVB homogeneous spin liquid described by the correlator

$$\mathscr{L}_{\mathbf{ij}}=\sum_{\sigma}\langle\phi_{\mathbf{ij}}^{\sigma}\phi_{\mathbf{ji}}^{\sigma}\rangle, \tag{20}$$

i.e., we use the second version of $H_{\rm int}$ in Eq. (13). Thus, the nonphysical states $|0\rangle$ and $|2\rangle$ are eliminated by the Hubbard procedure, since each fermion creation event at each site involves a projection operation in accordance with Eq. (14). This makes exchange vertex (13) more complicated; it can be described in the projection techniques by diagrams with twelve tails, as is shown by Fig. 1.

The role of projectors is to automatically eliminate a state with an opposite projection in creating a fermion with a given spin projection, and this guarantees that the creation operator acts on a state from the physical subspace $|\pm\rangle$. But, although correlator (20) is diagonal in subspace $|\pm\rangle$, the nonphysical states $|0\rangle$ and $|2\rangle$ manifest themselves as intermediate states in any attempt to describe the spin liquid in terms of fermion operators.

In Refs. 11 and 13 it was noted that introduction of a homogeneous RVB state in the mean-field approximation[16] violates the local gauge invariance due to constraint (4), (6), and long-wave fluctuations of gauge fields significantly change the character of RVB excitations in a two-dimensional Heisenberg lattice (see also Refs. 14, 35, and 36). In this paper, we do not consider the problem of long-wave fluctuations in gauge fields. We are interested primarily in nonlocal high-temperature magnetic fluctuations, which are also related, however, to the violation of the constraint.

As was shown in the fundamental study by Baskaran, Zou and Anderson,[16] the description of a uniform RVB state requires ''anomalous'' coupling between pseudofermions at different sites. It is clear that such a procedure drives the system beyond the physical space $|\pm\rangle$. The gauge theory of a spin liquid demonstrates that free propagation of a spinon is impossible. The complex shape of vertices in the projection technique (Fig. 1) indicates the same thing. Nonetheless,

we start construction of our scheme with a demonstration of how far this technique applies in the mean-field approximation; we then consider the possible effect of fluctuations on the mean-field solution.

Let us introduce an anomalous one-particle (one-fermion) temperature Green's function. In order to preserve particle–hole symmetry, let us express it in matrix form:

$$\hat{\mathscr{G}}_{\mathbf{ij}\sigma}(\tau)=-\langle T_\tau \hat{X}_{\mathbf{i}\sigma}(\tau)\hat{X}^+_{\mathbf{j}\sigma}(0)\rangle_{\tilde{H}}, \tag{21}$$

where

$$\hat{X}_{\mathbf{i}\sigma}=\begin{pmatrix} X_{\mathbf{i}}^{0\sigma} & X_{\mathbf{i}}^{\sigma 0} \\ \sigma X_{\mathbf{i}}^{-\sigma 2} & \sigma X_{\mathbf{i}}^{2-\sigma}\end{pmatrix}, \quad \hat{X}^+_{\mathbf{i}\sigma}=\begin{pmatrix} X_{\mathbf{i}}^{\sigma 0} & \sigma X_{\mathbf{i}}^{2-\sigma} \\ X_{\mathbf{i}}^{0\sigma} & \sigma X_{\mathbf{i}}^{-\sigma 2}\end{pmatrix}. \tag{22}$$

This Green's function has the structure

$$\hat{\mathscr{G}}_{\mathbf{ij}\sigma}(\tau)=-\begin{pmatrix} \langle T_\tau(X_{\mathbf{i}}^{0\sigma}(\tau)X_{\mathbf{j}}^{\sigma 0}(0) & \sigma\langle T_\tau(X_{\mathbf{i}}^{0\sigma}(\tau)X_{\mathbf{j}}^{2-\sigma}(0) \\ +X_{\mathbf{i}}^{\sigma 0}(\tau)X_{\mathbf{j}}^{0\sigma}(0))\rangle & +X_{\mathbf{i}}^{\sigma 0}(\tau)X_{\mathbf{j}}^{-\sigma 2}(0)\rangle \\ \sigma\langle T_\tau(X_{\mathbf{i}}^{-\sigma 2}(\tau)X_{\mathbf{j}}^{\sigma 0}(0) & \langle T_\tau(X_{\mathbf{i}}^{-\sigma 2}(\tau)X_{\mathbf{j}}^{2-\sigma}(0) \\ +X_{\mathbf{i}}^{2-\sigma}(\tau)X_{\mathbf{j}}^{-0\sigma}(0)\rangle & +X_{\mathbf{i}}^{2-\sigma}(\tau)X_{\mathbf{j}}^{-\sigma 2}(0)\rangle \end{pmatrix}. \tag{23}$$

The zero (one-site) matrix Green's function

$$\hat{g}_{\mathbf{i}\sigma}(\tau)=-\langle T_\tau \hat{X}_{\mathbf{i}\sigma}(\tau)\hat{X}^+_{\mathbf{i}\sigma}(0)\rangle_{\tilde{H}_0} \tag{24}$$

is diagonal, and its elements are

$$\begin{aligned} g^{(11)}_{\mathbf{i}\sigma}(\tau)&=-\langle T_\tau(X_{\mathbf{i}}^{0\sigma}(\tau)X_{\mathbf{i}}^{\sigma 0}(0)+X_{\mathbf{i}}^{\sigma 0}(\tau)X_{\mathbf{i}}^{0\sigma}(0))\rangle_0, \\ g^{(22)}_{\mathbf{i}\sigma}(\tau)&=-\langle T_\tau(X_{\mathbf{i}}^{-\sigma 2}(\tau)X_{\mathbf{i}}^{2-\sigma}(0) \\ &\quad +X_{\mathbf{i}}^{2-\sigma}(\tau)X_{\mathbf{i}}^{-\sigma 2}(0))\rangle_0. \end{aligned}$$

As in the previous case, the averaging $\langle\ldots\rangle_0\equiv\langle\ldots\rangle_{\tilde{H}_0}$ leaves the one-site Green's function in the physical sector of the Fock space. In particular,

$$\begin{aligned} g^{(11)}_{\mathbf{i}\sigma}(\tau_1-\tau_2)&=-\langle X_{\mathbf{i}}^{\sigma 0}(\tau_1)X_{\mathbf{i}}^{0\sigma}(\tau_2)\rangle_0 \\ &=-\langle X_{\mathbf{i}}^{\sigma\sigma}\rangle_0\ \exp[-i\sigma h(\tau_1-\tau_2)/2] \\ &\quad\times(\tau_1>\tau_2), \\ g^{(11)}_{\mathbf{i}\sigma}(\tau_1-\tau_2)&=\langle X_{\mathbf{i}}^{\sigma 0}(\tau_2)X_{\mathbf{i}}^{0\sigma}(\tau_1)\rangle_0 \\ &=\langle X_{\mathbf{i}}^{\sigma\sigma}\rangle_0\ \exp[-i\sigma h(\tau_1-\tau_2)/2](\tau_2>\tau_1). \end{aligned} \tag{25}$$

Unlike spin Green's functions (17), matrix elements of the function $\hat{g}_{\mathbf{i}\sigma}(\tau)$ formally represent the three-fermion loops containing one particle (spin up) and two hole (spin down) propagators, or one hole and two particle propagators. This function, however, can be simplified using the idempotence property of operator $b^\dagger b$, conditions (4) and (6), and Wick's theorem. By substituting the Hubbard operators in the interaction picture into Eq. (25), we obtain expressions for the elements of the one-site propagator,

$$g^{(11)}_{\mathbf{i}\uparrow}=\frac{1}{2}e^{-h\tau}\begin{cases} -\langle(1-n_{\mathbf{i}\downarrow})\rangle_0 & (\tau>0) \\ \langle n_{\mathbf{i}\downarrow}\rangle_0 & (\tau<0), \end{cases}$$

and a similar expression for the spin-down state.

One can easily check that the Green's function $\mathscr{G}^{(\alpha\alpha)}_{\mathbf{i}\sigma}$ is periodic, $\mathscr{G}_{\mathbf{ii}\sigma}(\tau<0)=-\mathscr{G}_{\mathbf{ii}\sigma}(\tau+1/T)$, so that by introducing the Matsubara frequencies $\omega_n=(2n+1)\pi T$ in the usual manner, we obtain

$$g^{(\alpha\alpha)}_{\mathbf{i}\sigma}(\omega_n)=\frac{1}{2}\,\frac{1}{i\omega_n+(-1)^\alpha\sigma h/2}. \tag{26}$$

The mean-field approximation[16] is based on the introduction of anomalous averages $\langle f^+_{\mathbf{i}\sigma}f_{\mathbf{j}\sigma}\rangle$. For the anomalous matrix Green's function (21), we must introduce four components:

$$\begin{aligned} \Delta^{11}_{ij\sigma}&=\langle X_{\mathbf{i}}^{\sigma 0}(\tau)X_{\mathbf{j}}^{0\sigma}(\tau'\to\tau)\rangle, \\ \Delta^{22}_{ij\sigma}&=\langle X_{\mathbf{i}}^{-\sigma 2}(\tau)X_{\mathbf{j}}^{2-\sigma}(\tau'\to\tau)\rangle, \\ \Delta^{12}_{ij\sigma}&=\langle X_{\mathbf{i}}^{\sigma 0}(\tau)X_{\mathbf{j}}^{-\sigma 2}(\tau'\to\tau)\rangle, \\ \Delta^{21}_{ij\sigma}&=\langle X_{\mathbf{i}}^{2-\sigma}(\tau)X_{\mathbf{j}}^{0\sigma}(\tau'\to\tau)\rangle, \end{aligned} \tag{27}$$

where $\Delta^{11}_{ij\sigma}=\Delta^{22}_{ij\sigma}$. Then one can easily check that the anomalous Green's function also satisfies a periodic condition like that in Eq. (21) on the inverse temperature. Thus, we can use the projection diagram technique in calculating the anomalous average $\Delta=\Sigma_\sigma\langle\phi^\sigma_{\mathbf{ij}}\rangle$, which characterizes a uniform RVB state. This ''order parameter'' can be derived from the relation

$$\Delta=\mathrm{Tr}(\hat{1}+\hat{\tau}_1)\hat{\mathscr{G}}_{\mathbf{ij}}(\tau\to-0), \tag{28}$$

where $\hat{1}$ and $\hat{\tau}_1$ are the Pauli matrices.

Let us rewrite Hubbard operators (10) in the particle–hole representation, $f_{\mathbf{i}\uparrow}\equiv a_{\mathbf{i}}$, $f_{\mathbf{i}\downarrow}\equiv b^+_{\mathbf{i}}$:

$$X_{\mathbf{i}}^{\uparrow 0}=a^+_{\mathbf{i}}b^+_{\mathbf{i}}b_{\mathbf{i}}, \quad X_{\mathbf{i}}^{2\downarrow}=a^+_{\mathbf{i}}b_{\mathbf{i}}b^+_{\mathbf{i}}, \quad X_{\mathbf{i}}^{\uparrow\downarrow}=a^+_{\mathbf{i}}b^+_{\mathbf{i}}\ldots$$

The mean-field approximation (28) corresponds to the following splitting of the interaction Hamiltonian H_{int}:

$$H_{\mathrm{MF}}=J\Delta\sum_{\mathbf{i}}\sum_{\mathbf{j}}^{\langle nn\rangle}(Y^{(h)}_{\mathbf{ij}}+Y^{(p)}_{\mathbf{ij}}), \tag{29}$$

where

$$\begin{aligned} Y^{(p)}_{\mathbf{ij}}&=a^+_{\mathbf{i}}b^+_{\mathbf{i}}b_{\mathbf{i}}b^+_{\mathbf{j}}b_{\mathbf{j}}a_{\mathbf{j}}+a^+_{\mathbf{i}}b_{\mathbf{i}}b^+_{\mathbf{i}}b_{\mathbf{j}}b^+_{\mathbf{j}}a_{\mathbf{j}}+a^+_{\mathbf{i}}b_{\mathbf{i}}b^+_{\mathbf{i}}b^+_{\mathbf{j}}b_{\mathbf{j}}a_{\mathbf{j}} \\ &\quad+a^+_{\mathbf{i}}b^+_{\mathbf{i}}b_{\mathbf{i}}b_{\mathbf{j}}b^+_{\mathbf{j}}a_{\mathbf{j}}, \\ Y^{(h)}_{\mathbf{ij}}&=b_{\mathbf{i}}a_{\mathbf{i}}a^+_{\mathbf{i}}a_{\mathbf{j}}a^+_{\mathbf{j}}b^+_{\mathbf{j}}+b_{\mathbf{i}}a^+_{\mathbf{i}}a_{\mathbf{i}}a^+_{\mathbf{j}}a_{\mathbf{j}}b^+_{\mathbf{j}}+b_{\mathbf{i}}a_{\mathbf{i}}a^+_{\mathbf{i}}a^+_{\mathbf{j}}a_{\mathbf{j}}b^+_{\mathbf{j}} \end{aligned}$$

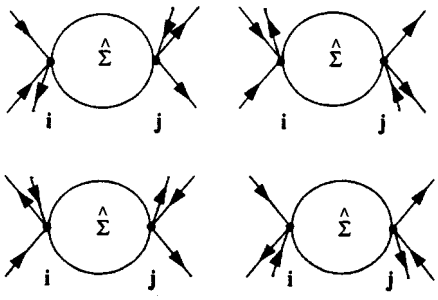

FIG. 2. Components of $\hat{\Sigma}$ matrix for the one-particle Green's function $\mathscr{G}_{\mathbf{ij}}$.

$$+ b_{\mathbf{i}} a_{\mathbf{i}}^{+} a_{\mathbf{i}} a_{\mathbf{j}} a_{\mathbf{j}}^{+} b_{\mathbf{j}}^{+} .$$

In terms of perturbation theory, this approximation can be described by the diagrams for the self-energy component $\hat{\Sigma}_{\mathbf{ij}}$ of Green's function (23) shown in Fig. 2. The four diagrams correspond to the four elements of $\hat{\Sigma}$. The Dyson matrix equation in this approximation is expressed by the diagrams in Fig. 3, in which double lines denote the one-site matrices $g_{\mathbf{i}\sigma}$, the dashed line denotes the Heisenberg exchange constant, and thick lines with two arrows denote the anomalous Green's function $\hat{\mathscr{G}}_{\mathbf{ij}\sigma}$. The Dyson equation

$$\hat{\mathscr{G}}_{\mathbf{ij}\sigma}(\omega_n) = \hat{g}_{\mathbf{i}\sigma}(\omega_n)\left(\delta_{\mathbf{ij}} + \sum_{\mathbf{l}} \hat{\Sigma}_{\mathbf{il}} \hat{\mathscr{G}}_{\mathbf{lj}\sigma}(\omega_n) \right) \tag{30}$$

is Fourier transformed to (as $h \to 0$)

$$2 i\omega_n \mathscr{G}_{\mathbf{k}\sigma}^{(\alpha\beta)}(i\omega_n) = \delta_{\alpha\beta} + J\Delta\varphi(\mathbf{k}) \sum_{\gamma} \mathscr{G}_{\mathbf{k}\sigma}^{(\gamma\beta)}(i\omega_n). \tag{31}$$

A solution of this equation system is

$$\mathscr{G}_{\mathbf{k}\sigma}^{(11)}(i\omega_n) = \frac{1}{2} \frac{i\omega_n - \epsilon_{\mathbf{k}}/2}{i\omega_n (i\omega_n - \epsilon_{\mathbf{k}})},$$

$$\mathscr{G}_{\mathbf{k}\sigma}^{(12)}(i\omega_n) = \frac{1}{2} \frac{\sigma\epsilon_{\mathbf{k}}/2}{i\omega_n (i\omega_n - \epsilon_{\mathbf{k}})}. \tag{32}$$

Here $\epsilon_{\mathbf{k}}$ is the spinon dispersion relation in the mean-field approximation in the form

$$\epsilon_{\mathbf{k}} = J\Delta\varphi(\mathbf{k}) \tag{33}$$

in the case of antiferromagnetic exchange only between nearest neighbors; $\varphi(\mathbf{k})$ is the corresponding form factor:

$$\varphi(\mathbf{k}) = \sum_{\mathbf{l}}^{(nn)} e^{i\mathbf{k}\cdot\mathbf{l}}. \tag{34}$$

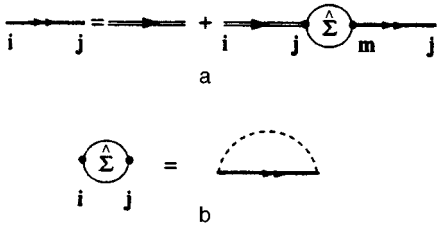

FIG. 3. (a) Dyson equation and (b) self-energy part of the Green's function $\mathscr{G}_{\mathbf{ij}}$ in the mean-field approximation.

By substituting Green's functions (32) into Eq. (28), we obtain a self-consistent equation for Δ:

$$\Delta = (ZN)^{-1} \sum_{\mathbf{k}} \varphi(\mathbf{k}) \tanh \frac{\beta[J\Delta\varphi(\mathbf{k}) - \mu]}{2}, \tag{35}$$

where Z is the coordination number. The chemical potential μ is treated as a Lagrange multiplier when constraint (4) is substituted into the Hamiltonian. This operation corresponds to substitution of $i\omega_n + \mu$ for $i\omega_n$. As usual, the local constraint can be replaced with a global one in the mean-field approximation:

$$N^{-1} T \sum_{\mathbf{k}} \sum_{\omega_n} \mathrm{Tr}(\hat{1} + \hat{\tau}_1) \hat{\mathscr{G}}_{\mathbf{k}}(i\omega_n) = 0. \tag{36}$$

By substituting Green's function (32) into Eq. (36), we obtain another self-consistency condition, which fixes μ at the mid-position of the spinon ''band,'' in accordance with particle–hole symmetry.

The ''phase transition'' temperature T^* at which a nontrivial solution for Δ emerges is given by

$$T^* = \frac{J}{2} (ZN)^{-1} \sum_{\mathbf{k}} \varphi^2(\mathbf{k}), \tag{37}$$

which is usually derived in the mean-field approximation using the functional integration technique (see, for example, Refs. 6, 37, and 38).

Thus, we have found that kinematic constraints on the pseudofermion representation of spin operators taken into account through Hubbard projection operators do not affect the mean-field solution for the RVB state as long as particle–hole symmetry is preserved at each step of the calculation. In this respect, the situation is different from that in which the same problem is solved by the Hubbard operator technique for the $t-J$ model with a finite density of holes,[39] where this symmetry is violated from the outset, since only doubly filled states $|2\rangle$ are excluded. In Ref. 22 another symmetry-based approach to elimination of nonphysical states is suggested, in which the ''fermion'' set $|0\rangle$, $|2\rangle$ is replaced with a unified ''boson'' vacuum $|V\rangle$.

Although the projection technique does not contribute any new features to the mean-field solution for the uniform RVB liquid, it offers, in principle, new opportunities for taking gauge fluctuations into account, which inevitably occur in spinon propagation. Moreover, as will be shown in the next section, in a three-dimensional Kondo lattice, spin liquid is formed in the neighborhood of the antiferromagnetic instability, because magnetic fluctuations are a decisive factor for both the transition temperature to the RVB state and the mechanism of this transition.

3. STABILIZATION OF SPIN LIQUID IN THE KONDO LATTICE AT HIGH TEMPERATURES. MEAN-FIELD APPROXIMATION

It is well known[40] that in the three-dimensional Heisenberg lattice the ground state energy of the RVB phase, E_{SL}, is higher than the antiferromagnetic state energy E_{AFM}. It has also been shown, however, that in the Kondo lattice described by the Hamiltonian (1), spin-flip scattering processes

can lead to stabilization of the RVB phase with respect to the magnetically ordered phase.[6,18] Since antiferromagnetic and spin-liquid correlations in the sf-exchange model are governed by the same coupling constant J_{RKKY}, the temperature at which the spin liquid is formed is close to the point of magnetic instability, $T^*-T_N<T_N$, so that antiferromagnetic correlations can significantly alter the character of a transition to the RVB phase, as compared to the results obtained in the mean-field approximation.

In order to describe formation of spin liquid in the Kondo lattice, we take Hamiltonian (1) in the original form

$$H_{\mathrm{eff}}=\sum_{\mathbf{k}\sigma}\ \varepsilon_k c^+_{\mathbf{k}\sigma}c_{\mathbf{k}\sigma}+\frac{1}{4}J_{sf}\sum_{\mathbf{i}}\ c^+_{\mathbf{i}\sigma}c_{\mathbf{i}\sigma'}f^+_{\mathbf{i}\sigma'}f_{\mathbf{i}\sigma}. \tag{38}$$

As mentioned in the Introduction, we operate in the range of parameters $\alpha\approx\alpha_c$ of Doniach's diagram,[3] in which all characteristic temperatures ($T_K\sim\varepsilon_F\exp(-1/2\alpha)$, $T_{N0}\sim\varepsilon_F\alpha^2$, and T^*, which is to be calculated) are of the same order of magnitude, so that in constructing the real phase diagram one must take into account the mutual effects of all three types of correlation—in particular, the change in the Néel temperature with respect to T_{N0} as given by simple perturbation theory in the parameter α.

As noted above, in this study we limit discussion to the range of high temperatures $T>T_K,T_{N0}$, in which the magnetic subsystem is a lattice of paramagnetic spins immersed in the Fermi sea of conductance electrons, and NCA applies to the one-site paramagnetic sf-scattering, i.e., each spin localized at a lattice site scatters conduction electrons independently of other spins. As the temperature is reduced, both Kondo scattering and correlations among lattice sites due to the indirect RKKY interaction are intensified.

The problem of competition between the indirect exchange among lattice sites and one-site sf-scattering has been discussed in literature many times, largely in terms of the Kondo problem with two impurities. In particular, Varma[41] analyzed the mutual influence of Kondo scattering and RKKY interaction at high temperatures by perturbation theory and concluded that the mutual influence of these two processes is small, at least in the leading logarithmic approximation in $\alpha\ \ln(\varepsilon_F/T)$. In this section, we will show that in the Kondo lattice, the effect of spin-flip scattering on magnetic correlations is a decisive factor for stabilization of the RVB phase in the critical region of Doniach's diagram, $\alpha\sim\alpha_c$.

In describing the intersite magnetic interaction under conditions of Kondo scattering in the noncrossing approximation (NCA), the effective vertex of the RKKY exchange $\tilde{J}_{\mathbf{ij}}(T,\epsilon)$ is determined by the diagram in Fig. 4a. In this diagram, dashed lines denote electron Green's functions, and the ingoing and outgoing lines correspond to pseudofermion operators. The one-site sf-exchange vertices Γ include loops corresponding to the leading logarithmic approximation in $\alpha\ \ln(\varepsilon_F/T)$ for the Kondo problem[3)] (Fig. 5). As a result, the effective interaction is given by

$$\tilde{J}_{\mathbf{ij}}(T,\varepsilon_m)=\Pi(R,\varepsilon_m)\Gamma^2, \tag{39}$$

where $\varepsilon_m=2m\pi T,\ R=|R_{\mathbf{i}}-R_{\mathbf{j}}|$.

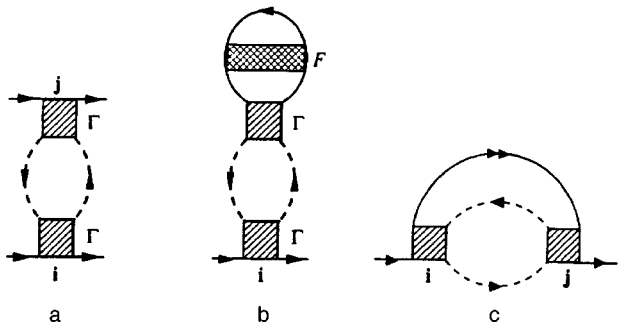

FIG. 4. (a) Effective vertex of renormalized RKKY interaction; self-energy part of the one-particle Green's function in the mean-field approximation (b) for the Néel and (c) RVB phase.

In the spirit of the logarithmic perturbation theory,[10] the argument of vertex Γ should contain only the highest input frequency, which is determined in our case by energies of electronic Green's functions included in the polarization loop $\Pi(R,\varepsilon_m)$ in the integral $\hat{J}_{\mathbf{ij}}(T,\varepsilon_m)$ (Eq. (39)). The polarization operator in the coordinate representation has the form

$$\Pi(\mathbf{R},\varepsilon_m)=T\sum_n\ D(-\mathbf{R},\omega_n+\varepsilon_m)D(\mathbf{R},\omega_n). \tag{40}$$

Since all heavy-fermion systems are characterized by large lattice constants, we use for electronic Green's functions $D(\mathbf{R},\omega_n)$ an expression asymptotic in p_FR:

$$D(R,\omega_n)=-\frac{p_F}{2\pi v_F R}\exp\left(-\frac{|\omega_n|}{2\varepsilon_F}p_FR+ip_FR\ \mathrm{sign}\ \omega_n\right), \tag{41}$$

so that the polarization operator takes the form

$$\Pi(R,\varepsilon_m)=\left(\frac{p_F}{2\pi v_F R}\right)^2 T\sum_{n=-\infty}^{n=\infty}\exp\left(-\frac{|\omega_n|}{v_F}R-\frac{|\omega_n+\varepsilon_m|}{v_F}R+ip_FR[\mathrm{sign}\omega_n+\mathrm{sign}(\omega_n+\varepsilon_m)]\right). \tag{42}$$

In the static limit,

$$\tilde{J}_R(T,0)=T\sum_n\ D^2(R,\omega_n)\Gamma^2(\omega_n,T). \tag{43}$$

The temperature dependence in Eq. (43) is largely determined by one-site vertices, and in the polarization loop one can use the condition $2\pi TR/v_f\ll 1$ and change summation over discrete frequencies to integration (see Appendix I). Then the exchange integral takes the form

FIG. 5. Parquet diagrams for effective vertex Γ.

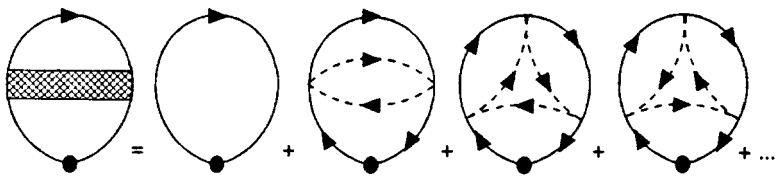

FIG. 6. Single-site diagrams describing Kondo screening of a localized spin.

$$\widetilde{J}_R(T,0)=2\left(\frac{p_F}{2\pi v_F R}\right)^2\cos(2p_FR)\times\int_{T\to 0}^{\infty}\frac{d\varepsilon}{2\pi}\exp\left(-\frac{\varepsilon}{\varepsilon_F}p_FR\right)\Gamma^2(\varepsilon,T). \quad (44)$$

This equation transforms to the standard RKKY exchange integral when modified vertices are replaced with the ''bare'' integrals, $\Gamma\to J_{sf}\Omega_0$, where Ω_0 is the elementary cell volume:

$$J_R^0=(J_{sf}\Omega_0)^2\Pi(R,0)=(J_{sf}\Omega_0)^2\frac{mp_F^4}{\pi^3}\times\left[\frac{\cos(2p_FR)}{(2p_FR)^3}+O\left(\frac{1}{(2p_FR)^4}\right]\right.$$
$$\equiv\left(\frac{J_{sf}^2}{\varepsilon_F}\right)\frac{(p_Fa_0)^6}{2\pi^3}\Phi(2p_FR). \quad (45)$$

Let us substitute into $\widetilde{J}_R(T,0)$ the vertex $\Gamma(\varepsilon,T)$ calculated in the leading logarithmic approximation, in accordance with diagrams given in Fig. 5 with the input frequency ε satisfying the condition $\ln(\varepsilon_F/\overline{\varepsilon})\gg 1$. For the characteristic energy $\overline{\varepsilon}\gg 1$, which determines integral (44) (see Appendix II), we find that the exchange parameter can be approximated by the function

$$\widetilde{J}_R(T,0)\approx\epsilon_F\frac{(p_Fa_0)^6}{2\pi^3}\left(\frac{J_{sf}}{\varepsilon_F}\right)^2\Phi(2p_FR)\times\left(1+2\alpha\,\ln\frac{T}{\varepsilon_F}\right)^{-n}. \quad (46)$$

The exponent n in this function depends on α and the argument of the oscillating function $\Phi(p_FR)$ (see the insert in Fig. 11). Thus, one can see that Kondo scattering has little influence on the form and spatial periodicity of the indirect exchange integral for $T>T_K$.[41] But this integral can be larger, and the larger the separation R between magnetic f-ions, the greater the increase.

In calculating the polarization operator and RKKY integral (46), we assumed that the electron Fermi surface was spherical. Note, however, that the exponent n in Eq. (46) is sensitive to the asymptotic behavior of the function $\Phi(2p_FR)$, so that the role of Kondo processes in intensification of the exchange turns out to be important in the case of a highly anisotropic Fermi surface. In the limiting case of a cylindrical Fermi surface,

$$\Phi(2p_FR)=-\left[\frac{\sin(2p_FR)}{(2p_FR)^2}+O\left(\frac{1}{(2p_FR)^3}\right)\right] \quad (47)$$

(see Appendix I), so that at the same value of p_FR, the integral $\widetilde{J}_R(T,0)$ is larger in the case of a cylindrical Fermi surface than in the case of a spherical surface.

Thus, the spin system can be described at $T>T_K$ by the effective RKKY Hamiltonian with the vertex shown in Fig. 4a in the nearest-neighbor approximation and under the assumption that the RKKY nearest-neighbor coupling has the antiferromagnetic sign. In the mean-field approximation, we treat the problem of stabilization of the spin liquid as a comparison between temperatures of transitions to the RVB state $[T^*(\alpha)]$ and to the antiferromagnetic state $[T_N(\alpha)]$ under conditions of sufficiently strong Kondo scattering, $\alpha\to\alpha_{c0}-0$, and the stabilization criterion is the inequality $T^*(\alpha)>T_N(\alpha)$. The function $T_N(\alpha)$ deviates from the quadratic function prescribed by the bare RKKY vertex. Along with the intensification of one-site vertices described by Eq. (46) and discussed above, there is a dynamic Kondo screening of localized spins, which is the reason for the suppression of antiferromagnetic order as $\alpha\to\alpha_{c0}$.

In the mean-field approximation, the transition temperatures $T_N(\alpha)$ and $T^*(\alpha)$ can be derived from the exchange vertex in Fig. 4a by closing spin-fermion lines, as shown in Figs. 4b and 4c, respectively. The first of these diagrams determines the molecular field for commensurate magnetic ordering characterized by the antiferromagnetic vector $\mathbf{Q}$ such that $\mathbf{Q}\cdot\mathbf{R}_{ij}=\pi$. The suppression of magnetic correlation by Kondo scattering is described by the vertex $F(T)$ in the diagram of Fig. 4b.[42,43] Summation of the set of logarithmic diagrams, the first of which are shown in Fig. 6, yields

$$F(T)=1-2\alpha\,\ln\frac{\varepsilon_F}{T}\Big/\ln\frac{T}{T_K}. \quad (48)$$

Although the function $F(T)$ deviates from this formula as $T\to T_K$,[44] and complete screening occurs only at $T=0$, the suppression of magnetic correlations compensates for the exchange intensification and thus reduces T_N as $\alpha\to\alpha_{c0}$.

The self-energy part of the one-site Green's function $\mathcal{G}_{\mathbf{ii}}$ (Eq. (21)), corresponding to the diagram of Fig. 4b, is

$$\Sigma_N(T)=\lambda\widetilde{J}(R,T)\langle S_z\rangle_T \quad (49)$$

(the factor λ is determined by the lattice configuration). Hence we derive for the mean spin

$$\langle S_z\rangle_T=\frac{1}{2}(\langle a_{\mathbf{i}}^+a_{\mathbf{i}}\rangle+\langle b_{\mathbf{i}}^+b_{\mathbf{i}}\rangle-1)$$

a self-consistent equation

$$\langle S_z\rangle_T=\frac{1}{2}F(T)\tanh\frac{\Sigma_N(T)}{2T}, \quad (50)$$

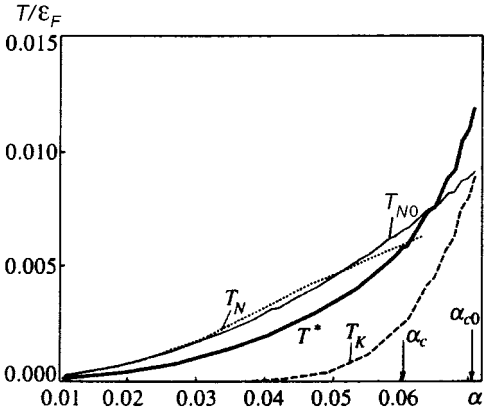

FIG. 7. Generalized Doniach diagram taking the RVB phase into account.

which is, naturally, the standard Brillouin equation for Weiss' molecular field taking Kondo screening into account.

The mean-field equation for Δ (Eq. (28)) is determined by the self-energy part of the anomalous Green's function $\hat{G}_{\mathbf{ij}}(\tau)$ (Eq. (23)) shown in Fig. 4c. This diagram can be substituted into the Dyson equation (Fig. 3), which in this case takes the form

$$\hat{G}(\mathbf{p},\omega_n)=g_0(\omega_n)\Bigg[1-2T\sum_m\sum_{\mathbf{q}}\tilde{J}(\mathbf{p}-\mathbf{q},\omega_n-\omega_m)\times\hat{G}(\mathbf{q},\omega_m)\hat{G}(\mathbf{p},\omega_n)\Bigg]. \tag{51}$$

Here $g_0(\omega_n)$ is the zero one-site Green's function with components (26), and $\tilde{J}(\mathbf{p}-\mathbf{q},\omega_n)$ is a Fourier transform of the indirect exchange integral (39), which in the nearest-neighbor approximation takes the form

$$\tilde{J}(\mathbf{q},\varepsilon_m)=\sum_{\mathbf{l}=0,\langle\mathbf{l}\rangle_{nn}}\tilde{J}_R(\varepsilon_m)e^{-i\mathbf{qr}}=\tilde{J}_0(\varepsilon_m)+\tilde{J}_R(\varepsilon_m)\varphi(\mathbf{q}). \tag{52}$$

The one-site integral $\tilde{J}_0(T,0)$ is estimated as $\alpha^2 T\ln(\varepsilon_F/T)$. Since this integral contains an additional small factor α at $T\sim T^*$, as compared to the intersite integral (46), it can be omitted.

By neglecting, as usual, the frequency dependence of the RKKY interaction, we obtain the mean-field equation (35) for Δ with the coupling constant $J=\tilde{J}_R(T,0)$. As follows from the configuration of the anomalous self-energy part (Fig. 4c), the screening effect responsible for suppression of local magnetic moments does not affect the mean-field parameter Δ, which can be naturally attributed to the singlet nature of the RVB-coupling. The Kondo ''screening'' radius can be estimated by high-temperature perturbation theory to be $\hbar v_F/2T_K$, which is much larger than the correlation radius of the singlet RVB pair, since electron scattering by these pairs is inefficient.

Calculations of the temperatures T^* and T_N by Eqs. (35), (46), (49), and (50) are given in Fig. 7 (see also Ref. 18). This graph shows that as $\alpha\to\alpha_{c0}$, these temperatures become closer, a new critical point α_c emerges in Doniach's diagram, on the right of which the RVB phase is stable with respect to the antiferromagnetic phase, and this stabilization takes place in the logarithmic neighborhood of the Kondo temperature. A calculation of T_N for $\alpha>\alpha_c$ makes no sense, because magnetic ordering in this region should follow another scenario.

Thus, we conclude that stabilization of a homogeneous RVB spin liquid in a three-dimensional Kondo lattice can occur only near the magnetic instability point under conditions of sufficiently strong Kondo screening of localized spins by conduction electrons. This result, obtained in the mean-field approximation, indicates that stabilization of the spin-liquid phase is incompatible with formation of Kondo singlet states characterized by anomalous averages $\langle c_i^+ f_i\rangle$,[6,45] since anomalous Kondo scattering is frozen at $T\approx T^*>T_K$. This resolves Nozières' well-known paradox[46] about the impossibility of screening all spins in the Kondo lattice by electrons from a thin layer of width T_K near the Fermi surface. In the scheme proposed above, the screening vanishes at sufficiently high temperatures above T_K, the Kondo temperature itself is not a singular point of the theory, renormalization of the sf-exchange integral is frozen at about $\tilde{J}(T^*)$, and at $T<T_K$, T^* electrons interact not with localized spins, but with spin-liquid excitations of the spinon type (see also Ref. 47).

In addition to the disadvantages related to violation of local gauge invariance, however, the mean-field approximation in the case of RVB coupling has another flaw, namely, it does not take into account the proximity of the spin system to the antifferomagnetic instability. In the following sections, we discuss possible consequences of this proximity for the RVB state, first in the self-consistent field approximation, then beyond this model.

4. EFFECT OF SPIN FLUCTUATIONS AND MAGNETIC ANISOTROPY ON RVB PHASE STABILIZATION

In the previous section, we determined that antiferromagnetic fluctuations inevitably turn out to be strong in an RVB spin liquid in the three-dimensional Kondo lattice at high temperatures $T\sim T^*$, and can lead, in principle, to magnetic ordering at $T\ll T^*$. Leaving this issue for subsequent studies, let us consider now the effect of spin fluctuations on features of the transition to the spin-liquid state in the mean-field approximation, but using its modification obtained through the projection technique, in which the order parameter is defined by Eq. (28). The diagram technique using Hubbard operators and developed in Sec. 2 allows us to take into consideration long-wave fluctuations of gauge fields due to the U(1) noninvariance of the RVB order parameter. Terms that take the phase of function Δ into account can be introduced into the effective Hamiltonian in standard fashion.[13,14] It is known that long-wave fluctuations in calibration fields do not lead to divergences destabilizing RVB averages in three-dimensional systems. Therefore, the introduction of such fluctuations reduces to the usual Fermi-liquid renormalizations with due account of the particle–hole symmetry condition. In two-dimensional Heisenberg lattices, however, fluctuations are important and must be taken into consideration.[13,14] In what follows, we do not discuss the

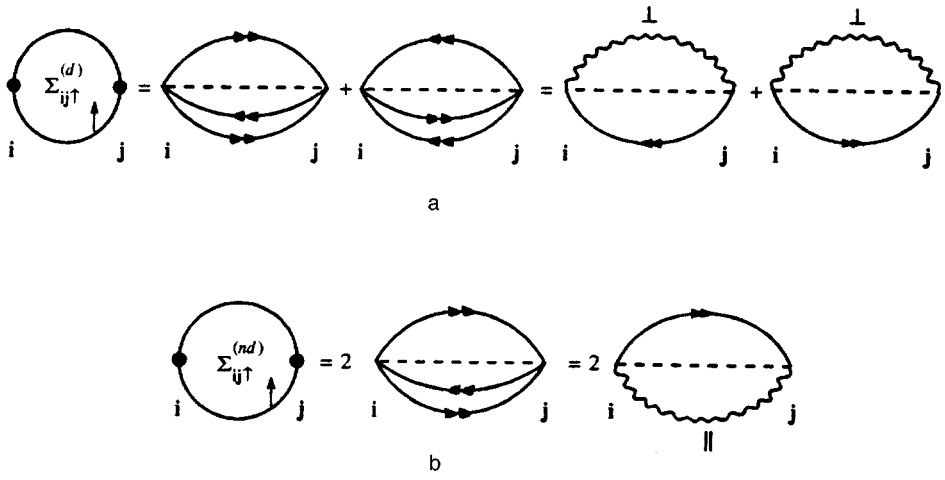

FIG. 8. Self-energy part for the anomalous propagator $\mathscr{G}_{ij}$, including the contribution of critical fluctuations in the mean-field approximation.

issue of long-wave fluctuations in gauge fields, and our analysis is limited to the mean-field approximation in a fixed calibration.

Having expressed the mean-field Hamiltonian in the form of Eq. (29), we considered in the subsequent calculations additional operators in $Y^{(p,h)}_{ij}$ as purely static projection operators, eliminating nonphysical states in thermodynamic averages. We now consider the fluctuation component of this ''kinematic'' interaction by transforming the effective mean-field spinon Hamiltonian for the Kondo lattice as follows:

$$H^{(\mathrm{RKKY})}_{\mathrm{MF}}=\tilde{J}\Delta\sum_{ij\sigma}\phi^{\sigma}_{ij}\equiv\tilde{J}\Delta\sum_{ij}\,(a^{+}_{i}K_{ij}a_{j}-a_{j}K^{+}_{ji}a^{+}_{i}+b_{i}K^{+}_{ij}b^{+}_{j}-b^{+}_{j}K_{ji}b_{i}). \tag{53}$$

Here $\tilde{J}$ is the renormalized constant of the RKKY interaction given by Eq. (46),

$$K_{ij}=S^{-}_{i}S^{+}_{j}-S^{z}_{i}S^{z}_{j}+\frac{1}{4},$$

and $K^{+}_{ij}=K_{ij}$. In the vicinity of the magnetic instability point, it is natural to consider operator K_{ij} as an operator describing critical excitations due to spinon propagation at temperatures close to T_N.

In order to obtain an expression for the spinon Green's function corresponding to this approximation, we reconsider the definition of its self-energy part. In the standard mean-field theory (Fig. 3), projection operators were included in the static approximation. The diagrams in Fig. 8 show how the diagonal and off-diagonal components of the self-energy part of the Green's function $\mathscr{G}_{ij}$, including transverse and longitudinal spin correlators, can be constructed from the vertices shown in Fig. 1. The lines with two arrows in Fig. 8 denote anomalous propagators

$$g^{\uparrow}_{ij}=-\langle T_{\tau}a_{i}(\tau)a^{+}_{j}(\tau')\rangle,$$
$$g^{\downarrow}_{ij}=-\langle T_{\tau}b_{i}(\tau)b^{+}_{j}(\tau')\rangle, \tag{54}$$

and wavy lines denote transverse and longitudinal correlation functions

$$\mathscr{K}^{\pm}_{ij}(\tau\to 0)=\langle T_{\tau}a^{+}_{j}(\tau+0)b^{+}_{j}(\tau+0)b_{i}(0)a_{i}(0)\rangle=\langle T_{\tau}S^{+}_{j}(\tau+0)S^{-}_{i}(0)\rangle,$$
$$\mathscr{K}^{zz}_{ij}(\tau\to 0)=\langle T_{\tau}b^{+}_{j}(\tau+0)b_{j}(\tau+0)b^{+}_{i}(0)b_{i}(0)\rangle=\frac{1}{4}-\langle T_{\tau}S^{z}_{j}(\tau+0)S^{z}_{i}(0)\rangle. \tag{55}$$

Unlike the fully anomalous Green's function (23), the anomalous functions (54) are one-particle propagators, while intersite spin correlators (55) are formed from projection operators. Now the sum of diagonal elements

$$\Sigma^{(d)}_{ij\uparrow}=\Sigma^{(11)}_{ij\uparrow}+\Sigma^{(22)}_{ij\uparrow}$$

in Eq. (28) is determined by the diagrams in Fig. 8a, while the contribution of off-diagonal elements

$$\Sigma^{(nd)}_{ij\uparrow}=\Sigma^{(12)}_{ij\uparrow}+\Sigma^{(21)}_{ij\uparrow}$$

corresponds to the diagrams in Fig. 8b. In deriving these expressions, we have used definition (3) and condition (6). Similar diagrams can be obtained for $\Sigma_{ij\downarrow}$. Summation of all these contributions in the mean-field approximation yields the effective Hamiltonian (53).

In the critical region $T_N<T<T^*$, the main contribution to spin correlators (53) is due to long-wave excitations with $\mathbf{k}\to 0$ and short-wave excitations with $\mathbf{k}\to\mathbf{Q}$ (see, for example, Ref. 48 and Sec. 5). The behavior of the response function $K(\mathbf{k})$ in the long-wave (hydrodynamic) limit $k\to 0$ is determined by fluctuations of the total magnetization of sublattices (which is zero in antiferromagnetic systems) and is diffusive in nature:

$$K^{R}(\mathbf{k},\omega)=K_{0}(\mathbf{k})\frac{iDk^{2}}{\omega+iDk^{2}}, \tag{56}$$

where

$$K_{0}(\mathbf{k})=\mathscr{K}(\mathbf{k},\omega=0)=\frac{\chi_{0}}{\tau+[1-J(\mathbf{k})/J(\mathbf{Q})]}\approx\frac{1}{2}\chi_{0}(T_N),$$

$$J(\mathbf{k})=J\sum_{\langle \mathbf{g}\rangle} e^{i\mathbf{kg}},\quad \chi_0(T)=\frac{S(S+1)}{3T},\quad \tau=\frac{T-T_N}{T_N} \tag{57}$$

(in Eq. (56) we have passed to the retarded Green's function for real frequency ω).

Near the antiferromagnetic vector $\mathbf{Q}$, the response function behavior is relaxation-like:

$$K^R(\mathbf{q},\omega)=\frac{1}{-i\omega/\Gamma\chi_0+K_0^{-1}(\mathbf{q})},\quad \mathbf{q}=\mathbf{k}-\mathbf{Q}, \tag{58}$$

where

$$K_0(\mathbf{q})=\mathscr{K}(q,\omega=0)=\frac{\chi_0}{\tau+(ql_0)^2} \tag{59}$$

is the Ornstein–Zernike static correlation function, and l_0 is the elementary excitation mean free path, which is comparable to the lattice constant.

In the mean-field approximation, we ignore the retardation of the RKKY interaction, and the diagrams in Fig. 8 yield for the self-energy

$$\tilde{\epsilon}_{\mathbf{k}}=\Sigma(\mathbf{k})=2\tilde{J}T^2\sum_{n,m\mathbf{q}}\sum_s \varphi(\mathbf{k}-\mathbf{q})g_{\mathbf{k}}(i\omega_n)\mathscr{K}^s_{\mathbf{q}}(i\varepsilon_m)$$

$$\approx\tilde{J}\Delta\left(\frac{\varphi(\mathbf{k})}{2}+2T\sum_{\mathbf{q}}\varphi(\mathbf{k}-\mathbf{q})K_0(\mathbf{q})\right). \tag{60}$$

Here s is the polarization index, while the anomalous Green's function $g_{\mathbf{k}}$ is expressed as $g_{\mathbf{k}}(i\omega_n)=(i\omega_n-\tilde{\epsilon}_{\mathbf{k}})^{-1}$. At high temperatures, we retain only the term with $\varepsilon_m=0$ in the sum over even Matsubara frequencies; then the spin Green's function $\mathscr{K}^s(\mathbf{q},0)$ in Fig. 8 has the same form in both the hydrodynamic and critical regions,[48] so that the main contribution to the spinon spectrum renormalization is due to the static susceptibility $K_0(\mathbf{q})$ (Eq. (59)).

The order parameter Δ defined by Eq. (28) and corresponding to the approximation of Eq. (53) and diagrams of Fig. 8 is given by

$$\Delta=\frac{1}{z}\sum_{\mathbf{pq}}\varphi(\mathbf{p}-\mathbf{q})\left[\frac{1}{2}\delta_{\mathbf{q},0}+2TK_0(\mathbf{q})\right]\tanh\frac{\tilde{\epsilon}_{\mathbf{p}}}{2T}. \tag{61}$$

Self-consistent equations (35) and (61) have been derived for the simplest case of isotropic exchange, which is, generally speaking, never realized in Kondo lattices. Therefore, before analyzing the effect of spin fluctuations on T^*, we generalize the mean-field theory to the case of anisotropic exchange. Let us introduce an exchange integral $J_{\mathbf{ij}}=\{J_\parallel,J_\perp\}$, where $J_\parallel$ and $J_\perp$ are the coupling constants for nearest neighbors in the basal plane and in the perpendicular direction, respectively. The degree of exchange anisotropy is measured by the parameter $\gamma=J_\perp/J_\parallel$. Now, instead of Hamiltonian (29) or (53), we must write the anisotropic mean-field Hamiltonian

$$H_{\mathrm{MF}}=\sum_{\mathbf{i},\rho_\perp}J_\perp\Delta_\perp Y_{\mathbf{i},\mathbf{i}+\rho_\perp}+\sum_{\mathbf{i},\rho_\parallel}J_\parallel\Delta_\parallel Y_{\mathbf{i},\mathbf{i}+\rho_\parallel}. \tag{62}$$

Here the anomalous averages $\langle Y_{\mathbf{i},\mathbf{i}+\rho_u}\rangle$, where $u=\perp,\parallel$, are derived from the equation system

$$\Delta_u=\frac{1}{z_u}\sum_{\mathbf{p}}\phi_u\left(\mathbf{p},\frac{T}{T_N},\gamma\right)\tanh\frac{\tilde{\epsilon}^u_{\mathbf{p}}(T/T_N,\gamma)}{2T} \tag{63}$$

with the dispersion relation

$$\tilde{\epsilon}^u_{\mathbf{p}}(T/T_N,\gamma)=J_u\Delta_u\phi_u(\mathbf{p},T/T_N,\gamma). \tag{64}$$

The structure factor $\phi_u(\mathbf{p},T/T_N,\gamma)$ renormalized by spin fluctuations can be expressed in terms of a structure factor $\varphi_u(\mathbf{p})$ like that in Eq. (33), where summation over nearest neighbors $\mathbf{l}$ is performed only in the basal plane ($\gamma<1$) or in the perpendicular direction ($\tilde{\gamma}=\gamma^{-1}<1$):

$$\phi_u\left(\mathbf{p},\frac{T}{T_N},\gamma\right)=\frac{1}{2}\varphi_u(\mathbf{p})+2T\sum_{\mathbf{q}}\varphi_u(\mathbf{p}-\mathbf{q})K_0(\mathbf{q}). \tag{65}$$

Index γ on the left-hand side of Eq. (65) is due to the anisotropic nature of correlator $K_0(\mathbf{q})$. Thus, the character of the transition to the spin-liquid state is determined by the degree of anisotropy: in the case of $\gamma<1$ spin-liquid correlations emerge first in the basal plane, and if $\gamma>1$ in the z-direction. At lower temperatures, the spin liquid naturally takes on three-dimensional properties, given that $\gamma\neq(0,\infty)$.

The transition temperature to the spin-liquid state, when spin fluctuations are taken into account, is determined by solving the equation

$$T_u^*=\frac{1}{2}\max\{J_\parallel,J_\perp\}\theta_u\left(\frac{T_u^*}{T_N},\gamma\right), \tag{66}$$

where

$$\theta_u\left(\frac{T_u^*}{T_N},\gamma\right)=(z_uN)^{-1}\sum_{\mathbf{p}}\phi_u^2\left(\mathbf{p},\frac{T}{T_N},\gamma\right), \tag{67}$$

$z_\parallel$ is the coordination number in the basal plane, and $z_\perp=2$.

In estimating the role of spin fluctuations for establishing the spin-liquid regime, it is convenient to introduce the temperature

$$T_u^{*(0)}=\frac{1}{2}\max\{J_\parallel,J_\perp\}\theta_u^{(0)} \tag{68}$$

of the transition to the RVB state in the anisotropic lattice without taking spin fluctuations into account. In this case,

$$\theta_u^{(0)}=(z_uN)^{-1}\sum_{\mathbf{p}}\varphi_u^2(\mathbf{p}). \tag{69}$$

Then the condition that the transition occurs by virtue of the spin-fluctuation mechanism is

$$\Upsilon_u(\gamma,T_u^{*(0)}/T_N)=\theta_u(T_u^{*(0)}/T_N,\gamma)/\theta_u^{(0)}>1. \tag{70}$$

The parameter $\Upsilon_u(\gamma)$ ($\Upsilon_u(\tilde{\gamma})$) for a simple cubic lattice is calculated in Appendix III. Critical values of the anisotropy parameters $\gamma_{1,2}$ at which the spin-liquid state stabilizes in almost one-dimensional and almost two-dimensional magnetic lattices are given for the case $T_u^{*(0)}/T_N=1$ in Fig. 9 for different values of τ. It is clear that only in a strongly anisotropic situation, almost one- or two-dimensional (see Eqs. (A.III.7) and (A.III.8)) spin correlations help formation of the spin liquid, and in the anisotropic case, inclusion of antiferromagnetic fluctuations in the mean-field approximation leads to suppression of the spin-liquid phase.

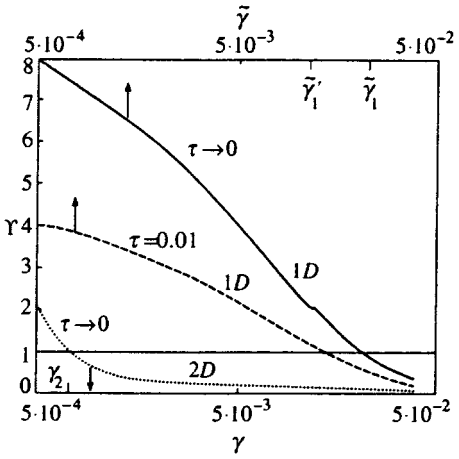

FIG. 9. Parameter Υ describing the effect of critical spin fluctuations on the transition temperature to the RVB phase for the quasi-one-dimensional ($1D$) and quasi-two-dimensional ($2D$) Kondo lattices. Parameter τ characterizes the proximity to the antiferromagnetic instability. The RVB state emerges at $\gamma<\gamma_1$ and $\tilde{\gamma}<\tilde{\gamma}_2$ in the cases of axial and plane magnetic anisotropy, respectively.

The analysis in this section once again indicates that the mean-field approximation is insufficient for the description of the spin liquid. In particular, even the diagrams of Fig. 8 indicate that the static approximation, generally speaking, does not apply to the critical region, since antiferromagnetic fluctuations define their own time and energy scales, which determine the real character of transition from the paramagnetic state to the spin-liquid state.

5. CRITICAL ANTIFERROMAGNETIC FLUCTUATIONS AND SPIN DIFFUSION

As mentioned in Sec. 4, in antiferromagnets critical fluctuations have differing properties in the long-wave ($k\to0$) and short-wave ($k\to Q$) regions, and the spin response function in these regions takes the form of Eqs. (56) and (58), respectively. The critical dynamics of antiferromagnets is usually analyzed using renormalization-group techniques applied to phenomenological models.[49,50] Chubukov[48] calculated the dynamic susceptibility of a two-dimensional antiferromagnet in the diffusion and relaxation regions using a diagram technique in the Schwinger boson representation. We investigate the dynamic susceptibility as a function of frequency and momentum in the thee-dimensional configuration using the pseudofermion technique.

In order to calculate the spin diffusion factor D and the relaxation constant Γ, we need to know, in addition to the spin correlators defined by the Larkin equation (19), the low-frequency behavior of the current correlator:

$$K_{\dot{S}\dot{S}}^{\alpha\beta}(\mathbf{k},\tau)=\delta_{\alpha\beta}\sum_{\mathbf{k}_1\mathbf{k}_2}V(\mathbf{k},\mathbf{p}_1)V(-\mathbf{k},-\mathbf{p}_2)\times\langle T_\tau(S^\mu_{\mathbf{p}_1+\mathbf{k}/2}S^\rho_{-\mathbf{p}_1+\mathbf{k}/2})_\tau(S^\mu_{-\mathbf{p}_2-\mathbf{k}/2}S^\rho_{\mathbf{p}_2-\mathbf{k}/2})_0\rangle, \tag{71}$$

where

$$V(\mathbf{k},\mathbf{p})=J(\mathbf{k}+\mathbf{p}/2)-J(-\mathbf{k}+\mathbf{p}/2).$$

FIG. 10. Self-energy part of the Green's function $\mathscr{G}_{\mathbf{ii}}$ including the contribution of critical fluctuations in the Born approximation.

There is an exact solution for the Fourier transform of correlator $K_{\dot{S}\dot{S}}$ continued to the upper half-plane expressed in terms of irreducible (noncuttable along the interaction line) self-energy parts of the spin and current correlation functions:

$$K^R_{\dot{S}\dot{S}}(\omega)=\Sigma^R_{\dot{S}\dot{S}}+\omega^2\frac{\Sigma^R_{SS}\mathscr{V}\Sigma^R_{SS}}{1-\Sigma^R_{SS}\mathscr{V}}. \tag{72}$$

Here $\mathscr{V}=(\Sigma^R)^{-1}-(K_0)^{-1}$ is the vertex part determined by the static response in the critical region.[19,51]

Using the Kramers–Kronig dispersion relations for retarded and advanced correlation functions, and the analytic properties of irreducible self-energy parts, one can derive from Eqs. (19) and (72) the expression

$$K^R_{SS}(\omega)=K_0\frac{\Gamma_{\mathbf{k},\omega}}{-i\omega+\Gamma_{\mathbf{k},\omega}}, \tag{73}$$

which holds as both $\mathbf{k}\to0$ and $\mathbf{k}\to\mathbf{Q}$.

The spin correlation functions can be expressed in terms of the pseudofermion Green's functions. For example, the expression for the one-site susceptibility has the form

$$\mathscr{K}^\perp_{\mathbf{i}}(\varepsilon_m)=T\sum_m\mathscr{G}_{\mathbf{ii}}(\omega_n+\varepsilon_m)\mathscr{G}_{\mathbf{ii}}(\omega_n), \tag{74}$$

(see Eq. (16)). Here $\mathscr{G}_{\mathbf{ii}}(\omega_n)$ is a Fourier component of the pseudofermion Green's function $\mathscr{G}_{\mathbf{ii}}(\tau)=\langle T_\tau f_{\mathbf{i}}(\tau)f^\dagger_{\mathbf{i}}(0)\rangle$. Since nonphysical states do not appear when calculating single-site averages for $S=1/2$, there is no need to introduce projection operators. As $T\to T_N$, scattering by the relaxation mode contributes a component described by the diagram in Fig. 10 to the self-energy part of the Green's function $\Sigma(\omega_n)$. Unlike the diagram of Fig. 8, here solid lines correspond to one-site propagators $\mathscr{G}_{\mathbf{ii}}$, and points to exchange vertices $\tilde{J}(\mathbf{q})$. The wavy line in this diagram corresponds to the spin Green's function (16) determined by the Larkin equation (19). In the absence of spin-liquid correlations, let us substitute into the self-energy part $\Sigma(\omega_n)$ of the pseudofermion Green's function the ''bare'' function $g_{i\sigma}$ from Eq. (26) and a spin function $\mathscr{K}(\varepsilon_m,\mathbf{q})$ in the form of a relaxator:

$$\Sigma(\omega_n)=\tilde{J}^2T\sum_m N^{-1}\sum_{\mathbf{q}}\varphi(\mathbf{q})^2\frac{1}{i(\varepsilon_m-\omega_n)}\frac{\Gamma\chi_0(T)}{|\varepsilon_m|+b(q)}, \tag{75}$$

where $b(q)=\Gamma[\tau+(ql_0)^2]$, and Γ should be calculated independently using the Dyson and Larkin equations. By calculating the sum over frequencies in Eq. (75) and continuing it analytically to the complex z plane, we obtain the following equation for poles of the pseudofermion Green's function:

$$z-\Sigma(z)=0,$$

$$\Sigma(z)=\sum_{\mathbf{q}} \frac{J^2\varphi^2(\mathbf{q})\mathscr{A}}{\pi}\frac{z}{z^2+b_{\mathbf{q}}^2}\left[\psi\left(-\frac{iz}{2\pi T}\right)-\psi\left(\frac{b_{\mathbf{q}}}{2\pi T}\right)-\frac{\pi T}{b_{\mathbf{q}}}+\frac{i\pi T}{z}\right], \tag{76}$$

where $\mathscr{A}=\Gamma\chi_0(T)$, and $\psi(y)$ is the digamma function. Hence, it is clear that the pseudofermion Green's function in this approximation is $\mathscr{G}^R_{\mathbf{ii}}(\omega)\sim[\omega+i\Gamma(T)]^{-1}$. By substituting this into Eq. (74), we find the one-site susceptibility

$$K^R_{\mathbf{i}}=\frac{\overline{\chi_0}}{1-i\omega/\Gamma}, \tag{77}$$

which is, in turn, can be substituted into the Larkin equation (which also includes, generally speaking, vertex corrections[48]), and thus the equation system for Γ and I_0 is closed.

The spin-liquid effects on the behavior of the spin correlation functions in the critical region can be accounted for by introducing anomalous intersite contributions into $\Sigma(\omega)$ (Fig. 10). Nonlocal fermion correlations lead to emergence of a new characteristic length characterizing short-range order, and change the temperature dependence of the static spin susceptibility and dynamic response functions. As a result, we have changes in the scaling behavior and in the frequency and momentum dependence of the spin susceptibility.

The spin diffusion factor is also determined by the self-energy part of the current correlator:[51]

$$D=\lim_{k\to 0,\omega\to 0}\frac{1}{k^2}\frac{\mathrm{Im}\Sigma^R_{\dot{S}\dot{S}}(\mathbf{k},\omega)}{\omega}K_0^{-1}(\mathbf{k}). \tag{78}$$

Since the behavior of the current correlator is fully determined by relaxation processes, effects of nonlocal spin correlations should also change scaling characteristics of the spin susceptibility in the hydrodynamic region.

The calculations described in this section are not considered a complete description of critical phenomena in antiferromagnets. These are instead illustrations given with the following aims: first, to demonstrate applicability of the suggested diagram technique to traditional problems of the theory of magnetic phase transition and, second, to outline feasible methods for taking into account the effect of spin-liquid correlations on antiferromagnetic fluctuations in the critical region.

6. CONCLUSIONS

In this paper, we have demonstrated that the spin-liquid state in the Kondo lattice can be more stable than the Kondo singlet state, owing to the same processes as those responsible for Kondo screening in the case of sufficiently strong antiferromagnetic sf-exchange. This rather paradoxical result can be explained by the fact that strong competition between Kondo scattering and spin-liquid correlations occurs at temperatures near the Néel point. Since all correlation effects at such temperatures have the same order of magnitude, the simple mean-field approximation cannot be used in describing the spin subsystem in a three-dimensional Kondo lattice.

The projection diagram technique suggested in the paper and based on the similarity between the Hubbard Hamiltonian for electrons and Heisenberg Hamiltonian for pseudofermions allows one, in principle, to go beyond the standard mean-field model of the homogeneous RVB phase.[6,16] Attempts to include antiferromagnetic fluctuations in the mean-field approximation (Sec. 4) do not produce any trustworthy results. Preliminary analysis, however, indicates[52] that the diagram technique suggested in the paper may allow one to manage without the mean-field approximation in describing effects which occur in the region of critical antiferromagnetic fluctuations and devise a more realistic scenario of emergence of the spin liquid in the Kondo lattice.

The investigation of spin diffusion near the Néel point reported in Section 5 indicates that the diagram techniques used in describing critical antiferromagnetic correlations at high temperatures may yield new physical results in the hydrodynamic region.

The authors are indebted to Yu. Kagan, N. V. Prokof'ev, G. G. Khaliullin, D. E. Khmel'nitskiĭ, and D. I. Khomskiĭ for helpful discussions and critical remarks. This work was supported by the Russian Fund for Fundamental Research (Project 95-02-04250a), INTAS (Project 93-2834), and Netherlands Organization for Support of Scientific Research (NWO, Project 07-30-002).

APPENDIX I

In calculating the polarization operator $\Pi(\mathbf{R})$ (Eq. (40)), we use the asymptotic form of the Green's function (41). Substituting it into Eq. (42), we obtain the expression for a spherical Fermi surface:

$$\Pi(R,\varepsilon_m)=T\left(\frac{m}{2\pi R}\right)^2\exp\left(-\frac{2|\varepsilon_m|}{v}R\right)\times\frac{\cos(2p_FR+i\varepsilon_mR/v)}{\sinh(2\pi TR/v)}+T\left(\frac{m}{2\pi R}\right)^2\times\exp\left(-\frac{|\varepsilon_m|}{v}R\right)\left[\frac{|\varepsilon_m|}{2\pi T}+\frac{\sinh(|\varepsilon_m|R/v)}{\sinh(2\pi TR/v)}\times\exp\left(-\frac{|\varepsilon_m|}{v}R+2ip_FR\ \mathrm{sign}\ \varepsilon_m\right)\right]. \tag{AI.1}$$

In the static limit, it reduces to

$$\Pi(R,0)=T\left(\frac{m}{2\pi R}\right)^2\frac{\cos(2p_FR)}{\sinh(2\pi TR/v)}=\frac{mp_F^4}{8\pi^3}\frac{\cos(2p_FR)}{(p_FR)^3}\left[1-\frac{\pi^2}{6}\left(\frac{T}{\varepsilon_F}p_FR\right)^2+\ldots\right], \tag{AI.2}$$

hence we have Eq. (45) at $T=0$.

In the case of a quasi-two-dimensional cylindrical Fermi surface

$$g(\mathbf{R},z,\omega_n)=\int\frac{d^3p}{(2\pi)^3}\frac{1}{i\omega_n-\xi(\mathbf{p})}\exp(i\mathbf{p}\cdot\mathbf{R}+ip_zz)$$

$$= \int_{-p_{z0}}^{p_{z0}} \frac{dp_z}{2\pi} e^{ip_z z} \int \frac{pdpd\varphi}{(2\pi)^2} \frac{1}{i\omega_n - \xi(\mathbf{p})} e^{i\mathbf{p}\cdot\mathbf{R}},$$

$$g(\mathbf{R},z,\omega_n) = \frac{\sin(p_{z0}z)}{\pi z} G(\mathbf{R},\omega_n). \tag{AI.3}$$

For $p_{z0} \gg p_F$ the effective RKKY interaction is independent of p_{z0},

$$J_{\mathrm{RKKY}}(\mathbf{R}) = \left(\frac{J}{\widetilde{n}_0}\right)^2 \Pi(\mathbf{R},0) = \left(\frac{J}{\widetilde{n}_0}\right)^2 \int \frac{d\omega}{2\pi} g^2(\mathbf{R},\omega)$$

$$= \left(\frac{J}{n_0}\right)^2 \int \frac{d\omega}{2\pi} G^2(\mathbf{R},\omega). \tag{AI.4}$$

Here $\widetilde{n}_0 = 4\pi p_F^2 p_{z0}/(2\pi)^3 = p_{z0}p_F^2/2\pi^2 = p_{z0}n_0/\pi$, $n_0 = p_F^2/2\pi$ is the two-dimensional density of electronic states, and $G(R,\omega_n)$ is the two-dimensional Green's function

$$G(R,\omega_n) = \int \frac{pdpd\varphi}{(2\pi)^2} \frac{1}{i\omega_n - \xi(\mathbf{p})} \exp(ipR\cos\varphi). \tag{AI.5}$$

Let us use the integral representation of the Bessel function

$$J_0(z) = \frac{1}{2\pi} \int_0^{2\pi} d\varphi \exp(iz\cos\varphi) \tag{AI.6}$$

in the asymptotic limit for large $|z|$:

$$J_0(z) \approx \sqrt{\frac{2}{z\pi}} \cos\left(z - \frac{\pi}{4}\right). \tag{AI.7}$$

Then we have

$$G(R,\omega_n) = -i\,\mathrm{sign}\,\omega_n \frac{m}{\sqrt{2\pi p_F R}} \exp\left(-\frac{|\omega_n|}{2\varepsilon_F} p_F R + i\left(p_F R - \frac{\pi}{4}\right)\mathrm{sign}\,\omega_n\right). \tag{AI.8}$$

Substituting this expression into Eq. (AI.4), we obtain

$$\Pi(R,\varepsilon_m) = -T\frac{m^2}{2\pi p_F R} \exp\left(-\frac{2|\varepsilon_m|}{v} R\right) \times \frac{\sin(2p_F R + i\varepsilon_m R/v)}{\sinh(2\pi TR/v)} - T\frac{m^2}{2\pi p_F R} \times \exp\left(-\frac{|\varepsilon_m|}{v} R\right) \left\{ \frac{|\varepsilon_m|}{2\pi T} - \frac{\sinh(|\varepsilon_m|R/v)}{\sinh(2\pi TR/v)} \exp\left[-\frac{|\varepsilon_m|}{v} R + 2i \times \left(p_F R - \frac{\pi}{4}\right)\mathrm{sign}\,\varepsilon_m\right]\right\}. \tag{AI.9}$$

In the low-temperature limit this expression becomes

$$\Pi(R,0) = -T\frac{m^2}{2\pi p_F R} \frac{\sin(2p_F R)}{\sinh(2\pi TR/v)}$$

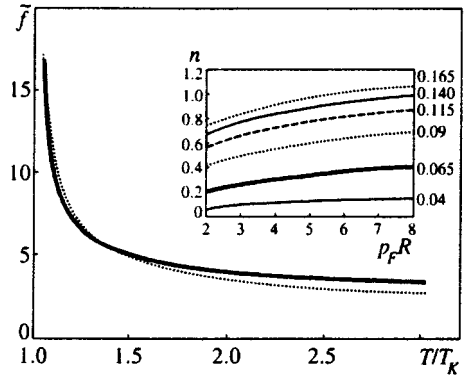

FIG. 11. Numerical values of integral $\widetilde{f}(p_F R)$ (solid line) and of the approximating function $f(p_F R)$ (see text).

$$= -\frac{mp_F^2}{4\pi^2} \frac{\sin(2p_F R)}{(p_F R)^2} \left[1 - \frac{\pi^2}{6}\left(\frac{T}{\varepsilon_F} p_F R\right)^2 + \ldots\right], \tag{AI.10}$$

and at $T=0$ to Eq. (47).

APPENDIX II

Intensification of the RKKY interaction due to Kondo renormalization of the single-site sf-exchange vertex, which is taken into account in the logarithmic approximation,

$$\Gamma(\varepsilon,\alpha) = \frac{1}{(1 + 2\alpha\,\ln(\varepsilon/\varepsilon_F))^2}, \tag{AII.1}$$

is described by the expression

$$f\left(p_F R, \alpha, \frac{T}{\varepsilon_F}\right) = \int_{T/\varepsilon_F}^{\infty} \frac{\exp(-p_F R x)dx}{(1 + 2\alpha\,\ln(x))^2}. \tag{AII.2}$$

The temperature dependence of this integral is determined by both Doniach's parameter α and the separation between neighboring Kondo centers (parameter $p_F R$).

If we neglect logarithmic renormalization (AII.1), the integral in (A.II.2) equals $1/p_F R$ for $T \ll \varepsilon_F/k_B$, and the integral in (44) reduces to the usual RKKY formula (45). When Kondo processes are taken into account, the function f defined by Eq. (A.II.2) can be approximated in the temperature range of interest, $[T_K, 3T_K]$, by the expression

$$f\left(p_F R, \alpha, \frac{T}{\varepsilon_F}\right) \approx \frac{1}{p_F R} \frac{1}{(1 - 2\alpha\,\ln(T/\varepsilon_F))^{n(p_F R,\alpha)}}, \tag{AII.3}$$

where the exponent $n = n(p_F R, \alpha)$ is independent of temperature. As a result, the high-temperature behavior of the RKKY interaction is determined by the function $\widetilde{f}(p_F R, \alpha, T/\varepsilon_F) = f(p_F R, \alpha, T/\varepsilon_F) p_F R$, which can be approximated as

$$\widetilde{f}\left(p_F R, \alpha, \frac{T}{\varepsilon_F}\right) \approx \frac{1}{(1 + 2\alpha\,\ln(T/\varepsilon_F))^{n(p_F R,\alpha)}}. \tag{AII.4}$$

Figure 11 shows the temperature dependence of the exact function $\widetilde{f}(p_F R = 5.0, \alpha = 0.09)$ calculated numerically (solid line) and the approximate function $\widetilde{f}(p_F R = 0.5, \alpha = 0.09)$ (dotted line) in the temperature range

$T_K<T<3T_K$. The exponent $n=n(p_FR,\alpha)$ of approximate function (AII.4) is shown in the insert as a function of p_FR in the range $2<p_FR<8$ for several values of α in the interval $0.04<\alpha<0.165$. The exponent was determined using the least-square fit in the temperature range $1.2T_K<T<3T_K$.

APPENDIX III

In this Appendix, we calculate the parameter Υ defined by Eq. (70), which characterizes the effect of spin correlations on the transition temperature to the RVB phase for a simple cubic lattice with anisotropic RKKY interaction due, for example, to a nonspherical Fermi surface. Let us introduce $J_\parallel \equiv J_x = J_y$ and $J_\perp \equiv J_z$. Then we must substitute into Eq. (57) for the spin correlator $K_0(\mathbf{q},\gamma)$ the parameter

$$j_q \equiv J_q/|J_Q| = -j_\parallel(\varphi_\parallel + \gamma\varphi_\perp), \tag{AIII.1}$$

where $\varphi_\parallel(q)=2(\cos q_x+\cos q_y)$, $\varphi_\perp(q)=2\cos q_z$, and $j_\parallel = J_\parallel/J_{\mathbf{Q}}$ $(a=1)$. To calculate sums in Eq. (65) like

$$T\sum_{\mathbf{q}} \varphi_u(\mathbf{p}-\mathbf{q})K_0(\mathbf{q},\gamma) = \frac{S(S+1)T}{6T_N j_0}\sum_{\mathbf{q}} \frac{\varphi_u(\mathbf{p}-\mathbf{q})}{T/T_N j_0 - j_{\mathbf{q}}/j_0}, \tag{AIII.2}$$

we use the integral representation for the spin correlator

$$K_0(\mathbf{q},\gamma) = \frac{S(S+1)j_{\mathbf{q}}}{6T_N j_0}\int_0^\infty dt\ \exp\left\{-\left(\frac{T}{T_N j_0}-\frac{j_q}{j_0}\right)t\right\}. \tag{AIII.3}$$

When the interaction in the basal plane is dominant $(\gamma<1)$, the spectrum of spin-liquid excitations has the form

$$\tilde{\epsilon}^{\parallel}_{\mathbf{p}}(T/T_N,\gamma) = \frac{1}{2}J_\parallel\Delta_\parallel\left[1-(2+\gamma)\frac{T}{T_N}A(\gamma,T/T_N)\right]\varphi_\parallel(q), \tag{AIII.4}$$

where the function $A(\gamma,T/T_N)$ can be expressed in terms of integrals of Bessel functions:

$$A(\gamma,\tau) = \int_0^\infty dt\ \exp\{-(2+\gamma)(1+\tau)t\}I_1(t)I_0(t)I_0(\gamma t). \tag{AIII.5}$$

Given that $\theta^{(0)}_\parallel = \theta^{(0)}_\perp = 1$ for the simple cubic lattice, we obtain

$$\Upsilon_\parallel(\gamma, T^{*(0)}_u/T_N) = [1-(2+\gamma)(1+\tau)A(\gamma,\tau)]^2/4. \tag{AIII.6}$$

When the interaction perpendicular to the basal plane is dominant $(\tilde{\gamma}<1)$, we have instead of Eqs. (A.III.4)–(A.III.6)

$$\tilde{\epsilon}^{\perp}_{\mathbf{p}}\left(\frac{T}{T_N},\gamma\right) = J_\perp\Delta_\perp\left[1-(1+2\tilde{\gamma})\frac{T}{T_N}\tilde{A}\left(\gamma,\frac{T}{T_N}\right)\right]\cos p_z, \tag{AIII.4$'$}$$

$$\tilde{A}(\tilde{\gamma},\tau) = \int_0^\infty dt\ \exp\{-(1+2\tilde{\gamma})(1+\tau)t\}I_1(t)I_0^2(\tilde{\gamma}t), \tag{AIII.5$'$}$$

$$\Upsilon_\perp(\tilde{\gamma}, T^{*(0)}_u/T_N) = [1-(1+2\tilde{\gamma})(1+\tau)\tilde{A}(\tilde{\gamma},\tau)]^2/4. \tag{AIII.6$'$}$$

Using asymptotic expressions for the integrals:

$$A(\gamma,\tau)|_{\gamma,\tau\to 0} \propto -\ln\max(\gamma,\tau),$$

$$\tilde{A}(\tilde{\gamma},\tau)|_{\tilde{\gamma},\tau\to 0} \propto [\max(\tilde{\gamma},\tau)]^{-1/2},$$

we obtain for the neighborhood of T_N in the case of strong anisotropy

$$\Upsilon_\parallel(\gamma, T^{*(0)}_u/T_N) \propto -\ln\max(\gamma,\tau), \tag{AIII.7}$$

$$\Upsilon_\perp(\tilde{\gamma}, T^{*(0)}_u/T_N) \propto [\max(\tilde{\gamma},\tau)]^{-1/2}, \tag{AIII.8}$$

and as a result, strong spin fluctuations stabilize the spin liquid.

[1)] Preliminary results of this study were given in the short note.

[2)] A procedure similar to that suggested below was described in Ref. 33 in the cases of the Anderson impurity and Anderson lattice. But since the Anderson Hamiltonian, unlike spin Hamiltonians (1) and (2), does not have local SU(2) symmetry, and the requirement of exact particle-hole symmetry is not imposed, there are many differences between formulations of rules of the diagram techniques.

[3)] Since in the case $S=1/2$ for one-site processes the constraint condition is satisfied automatically,[10] it is unnecessary to introduce projection operators.

[1] G. Zwicknagl, Adv. Phys. **41**, 203 (1992).
[2] A. C. Hewson, *The Kondo Problem to Heavy Fermions*, Cambridge University Press, Cambridge (1993).
[3] S. Doniach, Physica B **91**, 231 (1977).
[4] F. J. Ohkawa, Prog. Theor. Phys. Suppl. No. 108, 209 (1992).
[5] Y. Kuramoto and K. Miyake, Prog. Theor. Phys. Suppl. No. 108, 199 (1992).
[6] P. Coleman and N. Andrei, J. Phys.: Condens. Matter **1**, 4057 (1989).
[7] J. A. Millis and P. A. Lee, Phys. Rev. B **35**, 3394 (1987).
[8] Yu. Kagan, K. A. Kikoin, and N. V. Prokof'ev, Physica B **182**, 201 (1992).
[9] J. Gan, P. Coleman, and N. Andrei, Phys. Lett. **68**, 3476 (1992).
[10] A. A. Abrikosov, Physics **2**, 21 (1965).
[11] I. Affleck and J. B. Marston, Phys. Rev. B **37**, 3774 (1988).
[12] I. Affleck, Z. Zou, T. Hsu, and P. W. Anderson, Phys. Rev. B **38**, 745 (1988).
[13] L. B. Ioffe and A. I. Larkin, Phys. Rev. B **39**, 8988 (1989).
[14] P. A. Lee and N. Nagaosa, Phys. Rev. B **46**, 5621 (1992).
[15] S. Elitzur, Phys. Rev. D **12**, 3978 (1975).
[16] G. Baskaran, Z. Zou, and P. W. Anderson, Solid State Commun. **63**, 973 (1987).
[17] A. Ruckenstein, P. Hirschfeld, and J. Appel, Phys. Rev. B **36**, 857 (1987).
[18] K. A. Kikoin, M. N. Kiselev, and A. S. Mishchenko, JETP Lett. **60**, 358 (1994).
[19] Yu. A. Izyumov and Yu. N. Skryabin, *Statistical Mechanics of Magnetically Ordered Systems* [in Russian], Nauka, Moscow (1987).
[20] V. G. Bar'yakhtar, V. N. Krivoruchko, and D. A. Yablonskii, *Green's Functions in the Theory of Magnetism* [in Russian], Naukova Dumka, Kiev (1984).
[21] H. Keiter and G. Morandi, Phys. Rep. **109**, 227 (1984).
[22] F. Onufrieva and J. Rossat-Mignod, Phys. Rev. B **52**, 7572 (1995).
[23] D. C. Mattis, *The Theory of Magnetism*, Harper and Row, New York (1965).
[24] W. W. Lewis and R. B. Stinchcombe, Proc. Phys. Soc. London **92**, 1002 (1967).
[25] S. E. Barnes, J. Phys. F **6**, 1375 (1976).
[26] G. Kotliar and A. E. Ruckenstein, Phys. Rev. Lett. **57**, 1362 (1986).
[27] P. Coleman, E. Miranda, and A. M. Tsvelik, Phys. Rev. Lett. **70**, 2960 (1993).
[28] X.-G. Wen and P. A. Lee, Phys. Rev. Lett. **76**, 503 (1996).
[29] Y. Ono, T. Matsuura, and Y. Kuroda, Physica C **159**, 878 (1989).
[30] J. Hubbard, Proc. R. Soc. London, Ser. A **285**, 542 (1965).

[31] R. O. Zaitsev, Zh. Éksp Teor. Fiz. **70**, 1100 (1976) [Sov. Phys. JETP **43**, 574 (1976)].
[32] T. Yanagisawa, Phys. Rev. B **40**, 6666 (1989).
[33] J. Brinckmann, Europhys. Lett. **28**, 187 (1994).
[34] A. I. Larkin, Zh. Éksp. Teor. Fiz. **37**, 264 (1960) [Sov. Phys. JETP **10**, 186 (1960)].
[35] K. Kuboku, J. Phys. Soc. Jpn. **62**, 420 (1993).
[36] C. Mudry and E. Fradkin, Phys. Rev. B **49**, 5200 (1994).
[37] D. R. Grempel and M. Lavagna, Solid State Commun. **83**, 595 (1992).
[38] T. Tanamoto, H. Kohno, and H. Fukuyama, J. Phys. Soc. Jpn. **62**, 617 (1993).
[39] I. S. Sandalov and M. Richter, Phys. Rev. B **50**, 12855 (1994).
[40] P. W. Anderson, Mater. Res. Bull. **8**, 153 (1973).
[41] C. M. Varma, in *Theory of Heavy Fermions and Valence Fluctuations*, Springer Series in Solid-State Sciences, T. Kasuya and T. Saso (eds.), Vol. 62, Springer-Verlag, Berlin (1985), p. 277.
[42] K. Yosida and A. Okiji, Prog. Theor. Phys. **34**, 505 (1965).
[43] A. A. Abrikosov and A. A. Migdal, J. Low Temp. Phys. **3**, 519 (1970).
[44] A. M. Tsvelik and P. B. Wiegmann, Adv. Phys. **32**, 453 (1983).
[45] K. Miura, T. Ono, and K. Kuboku, Physica C **179**, 411 (1991).
[46] F. Nozières, Ann. de Phys. **10**, 1 (1985).
[47] K. A. Kikoin, J. Phys.: Condens. Matter **8**, 3601 (1996).
[48] A. Chubukov, Phys. Rev. B **44**, 392 (1991).
[49] B. I. Halperin and P. C. Hohenberg, Rev. Mod. Phys. **49**, 435 (1977).
[50] S. Chakraverty, B. I. Halperin, and D. Nelson, Phys. Rev. B **39**, 2344 (1989).
[51] S. V. Maleyev, Sov. Sci. Rev. A, I. M. Khalatnikov (ed.), Harwood Press, New York (1987), Vol. 8, p. 323.
[52] K. A. Kikoin, M. N. Kiselev, and A. S. Mishchenko, E-prints archive, Cond-Matt/96 08 121.

Translation was provided by the Russian Editorial office.